

REVIEW

Open Access



Diffusion weighted imaging and diffusion kurtosis imaging in abdominal oncological setting: why and when

Vincenza Granata^{1*}, Roberta Fusco², Andrea Belli³, Ginevra Danti^{4,5}, Eleonora Bicci⁴, Carmen Cutolo⁶, Antonella Petrillo¹ and Francesco Izzo³

Abstract

This article provides an overview of diffusion kurtosis (DKI) imaging in abdominal oncology. DKI allows for more data on tissue structures than the conventional diffusion model (DWI). However, DKI requires high quality images at b -values greater than 1000 s/mm² and high signal-to-noise ratio (SNR) that traditionally MRI systems are not able to acquire and therefore there are generally amplified anatomical distortions on the images due to less homogeneity of the field. Advances in both hardware and software on modern MRI scanners have currently enabled ultra-high b -value imaging and offered the ability to apply DKI to multiple extracranial sites. Previous studies have evaluated the ability of DKI to characterize and discriminate tumor grade compared to conventional DWI. Additionally, in several studies the DKI sequences used were based on planar echo (EPI) acquisition, which is susceptible to motion, metal and air artefacts and prone to low SNRs and distortions, leading to low quality images for some small lesions, which may affect the accuracy of the results. Another problem is the optimal b -value of DKI, which remains to be explored and not yet standardized, as well as the manual selection of the ROI, which could affect the accuracy of some parameters.

Keywords: Magnetic resonance imaging, DWI, DKI, Oncological setting

Introduction

Diffusion-Weighted Imaging (DWI) has been recognized as a significant magnetic resonance imaging (MRI) tool for disease assessment primarily in oncology [1–13]. The intensity, direction and time profile of the imaging gradient affect the diffusion sensitivity of water molecules and in DWI are included in a single simplified parameter called b -value (unit: s/mm²) [14–18]. The images acquired with different b -values were processed to obtain a parametric map that allows the quantification of the of the apparent diffusion coefficient that is linked to the microscopic mobility of water. In clinical setting, DWI

is performed using b -values up to 800–1000 s/mm², and the map quantification is performed using a monoexponential model considering that the diffusion water mobility follows a normal Gaussian model and then that the diffusion behaviour results in linear decay of the natural logarithm of the DWI signal intensity (SI) as the b -value increases and the slope represents the apparent diffusion coefficient (ADC) [19–24]. However, it is known that the water molecules diffusion within tissue follows a non-Gaussian model and for this reason in 2005 Jensen et al. [25] described a non-Gaussian approach, named Diffusion Kurtosis imaging (DKI) to assess tissue water diffusion coefficients. By means of the DKI it is possible to calculate the kurtosis median coefficient (MK), which assesses the variation of diffusion behaviour by a Gaussian, to a non-Gaussian model, and the diffusion coefficient (MD), which assesses the correction of

*Correspondence: v.granata@istitutotumori.na.it

¹ Division of Radiology, "Istituto Nazionale Tumori IRCCS Fondazione Pascale – IRCCS di Napoli", I-80131 Naples, Italy
Full list of author information is available at the end of the article



© The Author(s) 2022. **Open Access** This article is licensed under a Creative Commons Attribution 4.0 International License, which permits use, sharing, adaptation, distribution and reproduction in any medium or format, as long as you give appropriate credit to the original author(s) and the source, provide a link to the Creative Commons licence, and indicate if changes were made. The images or other third party material in this article are included in the article's Creative Commons licence, unless indicated otherwise in a credit line to the material. If material is not included in the article's Creative Commons licence and your intended use is not permitted by statutory regulation or exceeds the permitted use, you will need to obtain permission directly from the copyright holder. To view a copy of this licence, visit <http://creativecommons.org/licenses/by/4.0/>. The Creative Commons Public Domain Dedication waiver (<http://creativecommons.org/publicdomain/zero/1.0/>) applies to the data made available in this article, unless otherwise stated in a credit line to the data.

the non-Gaussian bias [25–27]. The term dimensionless kurtosis describes the degree of deviation from the Gaussian distribution of the spin displacements along the observation axis and therefore, when the average over all directions is calculated, the mean kurtosis is obtained. The MD value provides novel diffusion properties that describe the tissue microstructure.

DKI allows for more data on tissue structures than the conventional diffusion model (DWI). However, DKI requires high quality images at b -values greater than 1000 s/mm^2 and high signal-to-noise ratio (SNR) that traditionally MRI systems are not able to acquire and therefore there are generally amplified anatomical distortions on the images due to less homogeneity of the field. Advances in both hardware and software on modern MRI scanners have currently enabled ultra-high b -value imaging and offered the ability to apply DKI to multiple extracranial sites [28–44].

Hence, radiologists could benefit through a better understanding of the major concepts of DKI.

In this paper, we evaluate the basic principles of DKI and clinical applications in oncological setting within the recent peer-reviewed literature.

Diffusion analysis: basic principles

DKI analyses non-Gaussian water diffusivity using a polynomial approach according to the following equation:

$$S_i = S_0 * e\left(-b_i * D_{app} + 1/6 + b_i^2 * D_{app}^2 * K_{app}\right)$$

In this, there are two variables, D_{app} and K_{app} , while S_0 is the basal signal with b value = 0.

K_{app} is the apparent diffusional kurtosis, which reflects the higher distribution of the high tissue diffusivities that occurs in the setting of the non-Gaussian diffusion behaviour. K_{app} is determined by the curvature of the SI decay away from the plot that would be predicted by a monoexponential model. The D_{app} is the diffusion coefficient corrected to take into account the observed non-Gaussian behaviour and is determined by the slope of the SI decay diagram.

The DKI approach offers radiologists the possibility of obtaining information on the anisotropic characteristics of tissues not obtainable with conventional DWI [27].

Tissue ADC at b -values below 1000 s/mm^2 has been recognized as an assessment primarily of the extracellular space [27]. Cell arrangement, cell size distribution, cell density, extracellular space viscosity, glandular structures, and membrane integrity are all variables that can affect the diffusion of water into the extracellular space. Hence, lower ADC values have often been attributed to higher cell density. In contrast, K_{app} has been sized to exemplify the direct relationships of water molecules to

cell membranes and intracellular complexes, although it is also influenced by other hard-to-separate extracellular parameters [27]. In fact, at the nanoscopic level, water is an inhomogeneous substance due to the polar nature of its molecule. Furthermore, water molecules could form 3D arrays in the presence of interfaces with charged materials such as polarized cell membranes or organelles or protein molecules, resulting in organization in layers with reduced diffusivity [27]. In this scenario, DKI values have a higher specificity to reveal water interactions within cell and tissue components [27].

Acquisition consideration

DKI is acquired using a standard DWI sequence also using ultra high b -values. Conventional DWI should require acquiring only two b -values for ADC evaluation while DKI should require at least three different b -values since there is an additional variable (K_{app}) within the mathematical model. The possibility of acquiring more than three b -values and at least two b -values above and below 1000 s/mm^2 should be considered to help capture non-Gaussian behaviour [27].

To obtain accurate DKI values, it is critical that high b -values have adequate SNR. However, this, at higher b -values, is remarkably challenging in body imaging, given the faster signal decays and the penchant for employing faster sequences. Therefore, it may be necessary to reduce the spatial resolution or increase the number of signal averages to maintain SNR [27].

Today, MR systems do not habitually offer in-line DKI post-processing options. Therefore, separate post-processing software are needed. At least, DKI assessment should offer two maps (D_{app} and K_{app}). D_{app} map is similar to ADC map. Reductions in D_{app} are usually correlated with increases in K_{app} , both indicating abnormal diffusion behaviour in similar anatomic sites. However, a visual analysis of the two maps could be diagnostically not sufficient. Instead, quantitative evaluation is suggested to fully harness the complementary role of kurtosis in distinguishing tissue pathology [27].

Clinical studies

In oncological setting, the interpretation of images comprises different phases of patient management (diagnosis, staging, and assessment of treatment response) [45–54]. The spread in expertise in cancer and the opportunity to obtain a tailored treatment by choosing a proper approach, as well as the management of patients within a multidisciplinary team has increased the patient prognosis [55–69]. In this scenario, the possibility to use a diagnostic tool that evaluates cancer characteristics at microscopic level explains the reasons for the great attention on DWI [70–76].

By quantifying the non-Gaussianity of the diffusion distribution in DWI, Kapp is a comparatively direct measure of the heterogeneity of the tissue microstructure. Recent studies have reported that DKI can reflect microstructural conditions more accurately than conventional DWI [77, 78]. These promising results ignite an interest in DKI that may allow for more comprehensive tissue characterization than conventional DWI.

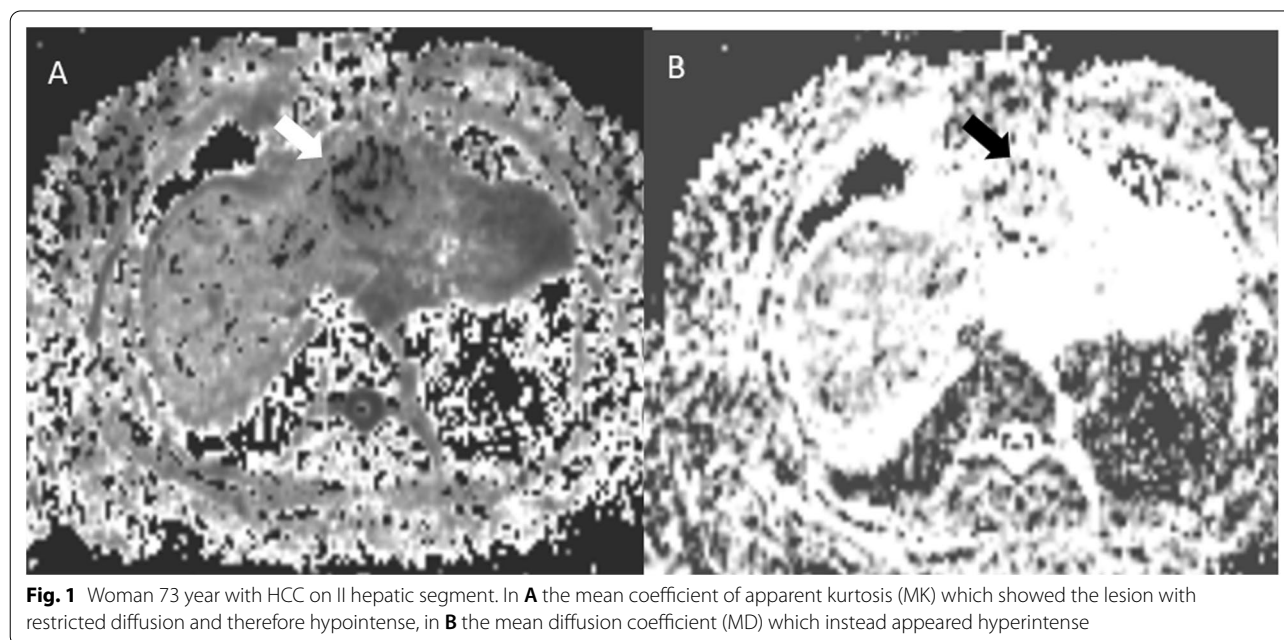
Liver

Several researches have assessed the role of DKI in liver diseases, with particular regard in fibrosis and hepatocellular carcinoma (HCC), comprising different phases of patient management (Fig. 1).

Generally, hepatic fibrosis is represented as a reaction to a disorder associated with hepatocellular degeneration [79–84]. The amount of fibrous connective tissue increases due to the progression of inflammatory diseases with cellular degeneration or necrosis. During the process of fibrosis, molecules of collagen, glycosaminoglycans and proteoglycans are deposited in the extracellular space of the liver. Consequently, hepatic fibrosis accompanied by swelling of the hepatocytes and infiltration of inflammatory cells narrows the extracellular space, increasing the average value of kurtosis. Yoshimaru et al. [79] evaluated the relationship between DKI and liver function by comparing the mean value of kurtosis with the Child–Pugh score, the ALBI score and the ICG-R15 value, which are typical indicators of liver function [80] and demonstrating that liver function can be quantitatively assessed using the mean kurtosis value. Indeed,

the fibrotic process could explain the positive correlation between the mean value of kurtosis and the Child–Pugh score or the ALBI score. However, there was little correlation between the mean value of kurtosis and the Child–Pugh score or the ALBI score presumably because the pattern of variation of the DKI and Child–Pugh scores or the ALBI scores differ according to the state of the hepatocyte tissue and liver function, respectively.

Recently, several studies have evaluated the role of DKI in HCC for the characterization and evaluation of the response to treatment [1, 83, 85–90]. However, the consistency and repeatability of the adapted parameters have not been assessed. It is known that more complex models with multiple parameters tend to oversize the data, resulting in poor repeatability and limited use in clinical practice. Furthermore, in order to capture the non-Gaussian diffusion behaviour of water molecules in biological tissues, maximum b -values of about 2000 s/mm² have been proposed for the liver. A higher b -value means a lower SNR and less repeatability of the calculated parameters. Therefore, it is necessary to explore whether or not non-mono-exponential models may provide desirable repeatability of measurements for HCC. Rosenkrantz et al. [77] performed the DKI assessment in HCC using fresh liver explants. Twelve liver explants underwent MR study using a sequence with a maximum b value of 2000 s/mm². A conventional mono-exponential model was used to calculate the ADC and a non-Gaussian model to evaluate Kapp and Dapp. They showed that 16 HCC had intermediate to substantial excess diffusional kurtosis and Dapp was 23% greater than ADC



medium. ADC, Dapp, and Kapp had significant differences between responding and non- or partially responding lesions. Among the unresponsive nodules, cellularity showed a strong inverse association with ADC, a weaker inverse association with Dapp, and a direct association with Kapp [77].

With regard to prognosis, the pathological grade of HCC and microvascular invasion (MVI) are main involved features, since they are independent predictive features for recurrence and long-term survival after resection [91–94]. Cao et al. explored the performance of DKI in predicting the presence of microvascular invasion (MVI) and the histological grade of HCC and compared it to the conventional ADC value. The results of their study suggested that of all the diffusion parameters studied, MK might be the most promising factor in the systematic assessment of tumour biological behaviours and serve as an independent risk factor for early relapse after liver resection within one year [95]. Wang et al. [96] that showed the correlation between MK and histological grade of HCC have confirmed these results.

Few studies have evaluated DKI and liver metastases. Granata et al. assessed the role of DKI in patients with colorectal liver metastases to detect RAS mutation [97]. They showed a significant association between the group with RAS mutation and the group without RAS mutation with MK [MK standard deviation (STD)], MD, and the perfusion fraction (FP). The best results were reached by MK STD with an area under curve (AUC) of 0.80, an accuracy of 79% using a cut-off of 203.90×10^{-3} [97].

Ablative treatment is a minimally invasive approach that is usually used in the treatment of tumours [98–101]. Ablation treatment is believed as a potential first-line tool in small HCCs (<3 cm) [101]. The goal of ablative treatment is necrosis. Therefore, tumour volume decrease may be absent with these treatments. Tumour features such as angiogenesis and hypoxia are more pertinent to assessing response, so as it is necessary to develop new functional biomarkers. Goshima et al. [87] assessed DKI and conventional DWI for evaluating treatment response in hypervascular HCC. Sixty-two patients (112 HCCs; viable, $n=63$; non-viable, $n=49$); underwent MRI; DKI was performed with different b values: 0, 100, 500, 1000, 1500, and 2000s/mm². The MK and ADC values of the hepatic parenchyma and of the HCCs were assessed. The detectability of viable HCC based on MK and ADC was analysed. They also evaluated the correlation between Child–Pugh classes and MK or ADC values. The MK value was significantly higher for the viable lesions than for the non-viable lesions, while ADC values were significantly lower between the viable lesions and non-viable lesions. Considering that viable HCCs are characterized by structural complexity, with higher cellularity with

nuclear atypia, more vascular hyperplasia or necrosis, and occasionally fatty deposition, it is known that DKI model represents better the complexity of biological tissues. However, it is essential that DKI might be evaluated in a reproducible manner and therefore is mandatory to standardize the protocol, establishing the strength and number of “ b ” values, the model to evaluate quantitative parameters [87].

Pancreas

Diagnosis of pancreatic cancer remains challenging, due to overlapping imaging features with benign lesions (Fig. 2). However, an accurate detection and characterization of lesions is required since the prognosis is connected to tumor type and grade, so as it is required a correct staging. Thus, an imaging tool that provides higher tumor conspicuity would be needed to enhance staging and clinical outcomes [102–105]. Granata et al. [106] assessed functional MRI features to differentiate pancreatic tumours, perilesional inflammatory tissue, and normal parenchyma. They used dynamic contrast-enhanced MRI (DCE-MRI), DKI, intravoxel incoherent motion (IVIM), and conventional DWI-derived parameters showing that MD by DKI, could be helpful for the differentiation of lesion to normal parenchyma and perilesional inflammation.

Shi et al. [107] assessed MRI performance in differentiating pancreatic ductal adenocarcinomas (PDACs), from solid pseudo papillary neoplasms (SPNs) and pancreatic neuroendocrine tumors (PNETs) using DKI. Considering that therapeutic strategies differ significantly between PDACs, and SPNs and PNETs, since for PDACs, aggressive surgical approaches such as the Whipple technique with extensive lymph node dissections is usually used, which entails higher post-surgical complications, it is crucial a pre-surgical staging in order to plan the more appropriate technique. The researches [107] showed that the accuracy rate with DKI for differentiating PDAC from SPNs and PNETs was higher than that of subjective diagnosis alone ($P<0.05$) so that DKI could assist radiologists in accurately diagnosis.

Electrochemotherapy (ECT) is an interesting approach for treatment of several tumours [108–112]. This technique links the administration of drugs with electric pulses for cell membrane electroporation and it is efficacy and safety in the treatment of PDCA [113]. However, the correct assessment of this treatment is a challenge for radiologists since tumour necrosis is not associated with a dimensional change. In this scenario, the response evaluation criteria in solid tumour (RECIST) are not adequate. Granata et al. assessed Conventional DWI and DKI as tools to evaluate treatment efficacy. They showed

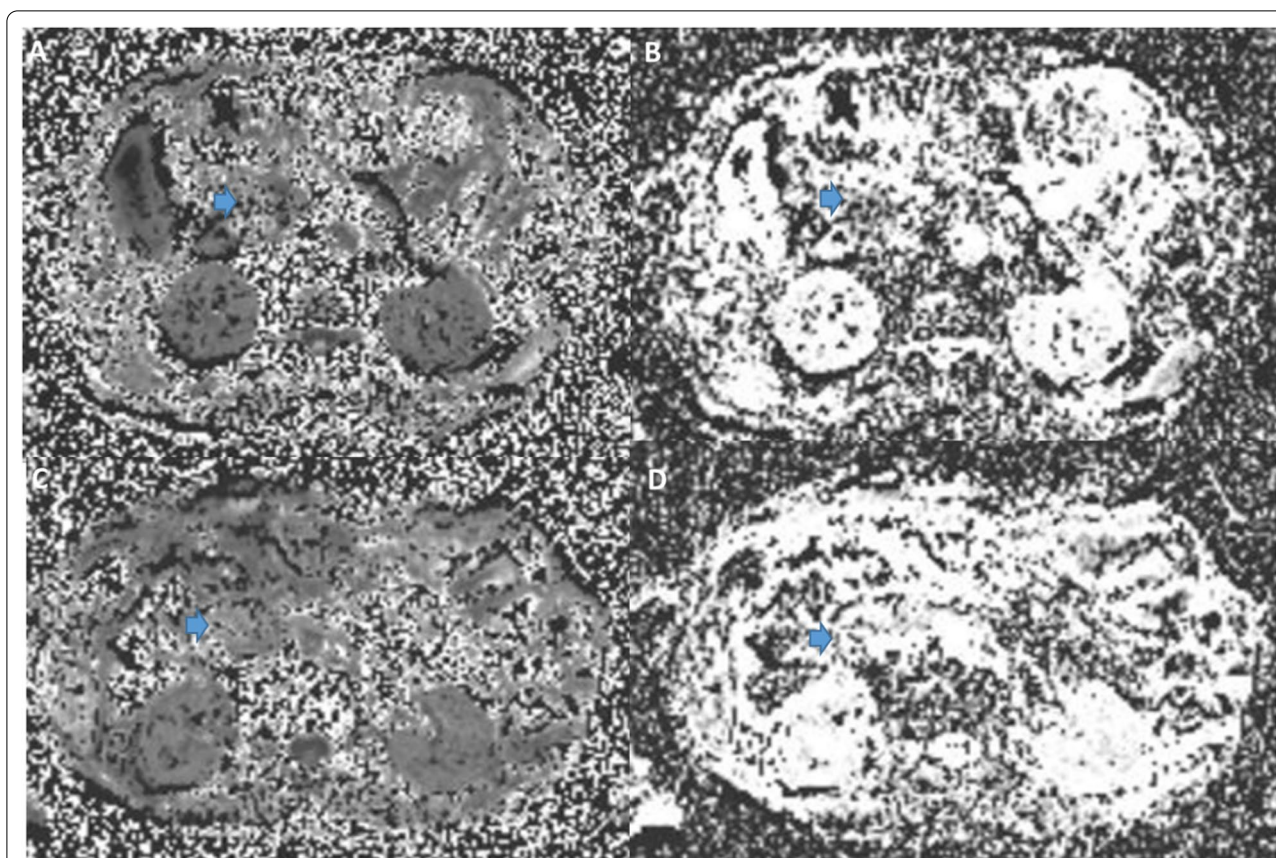


Fig. 2 Adenocarcinoma of the pancreatic head. MK map before and after treatment (**A, C**); MD map before and after treatment (**B, D**). In MK map can be observed a reduction of signal intensity while in MD map can be observed an increase of intensity. In both cases the variation of intensity was linked to a good response after the treatment

that MD improved the diagnostic performance respect to ADC in the response assessment [114].

Rectal cancer

Although rectal cancer is one of the most common tumour worldwide and, though in order to identify the lesion as soon as possible, there were a widespread use of screening, however, to day, this cancer is still diagnosed in an advanced stage of the disease [115–118]. Nowadays, the standard of care in patients with locally advanced rectal cancer (LARC) is still preoperative chemoradiotherapy (pCRT) followed by total mesorectal excision [119–122], though in-patient with a complete response to treatment, it is possible to consider a “wait-and-watch” strategy.

Conventional o morphological (m)-MRI, based on T2-W sequences, is at present believed the main imaging toll for staging. However, conventional sequences have some weaknesses, particularly after pCRT. To surmount this limit, functional data have been evaluated [123–132] (Fig. 3).

The managing of rectal cancer patient is largely founded on the recurrence risk stratification. Prognostic signs involve TNM stage, histological grade, peritumonic lymphovascular invasion (LVI) or neural invasion, circumferential margin (CRM) involvement [128]. Zhu et al. [133] evaluated DKI ($b\text{-value} > 2100 \text{ s/mm}^2$) and conventional DWI ($b\text{-value} > 1000 \text{ s/mm}^2$) in 56 rectal cancers, evaluating the relationship between kurtosis, diffusivity, ADC with pT and pN stages and histological degrees. Kurtosis was significantly higher in tumors with nodal involvement than in those without nodal involvement. Furthermore, kurtosis was significantly higher in high-grade than low-grade tumors, while no significant differences in diffusivity or ADC were found between low- and high-grade tumors. Cui et al [134] evaluated the associations between conventional DWI (highest $b\text{-value}$ 1000 s/mm^2) and DKI (highest $b\text{-value}$ 2100 s/mm^2) and plasma carcinoembryonic antigen level, pT stage, pN stage, grade tumor, peritumor LVI or neural invasion and CRM invasion in 79 patients with LARC, demonstrating that kurtosis was greater in patients with lymph node

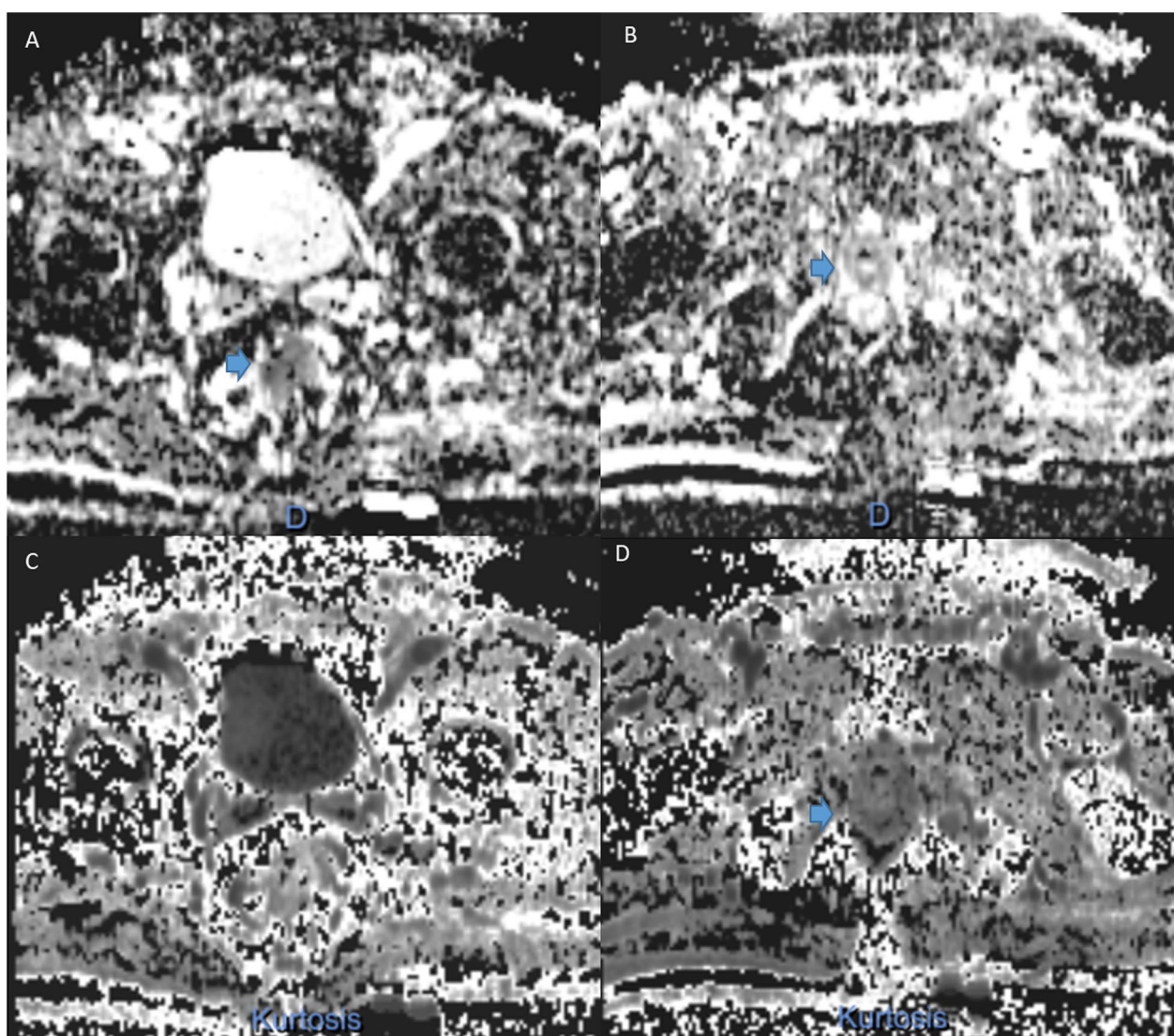


Fig. 3 DKI-derived parameters maps pre (A, C) and post-treatment (B, D) for a responder patients (TRG 2): MK A and B, MD C, D. In MK map can be observed a reduction of signal intensity while in MD map can be observed an increase of intensity. In both cases the variation of intensity was linked to a good response after the treatment

and CRM involvement, low grade lesion and presence of LVI. ADC and diffusivity were significantly correlated at stages T and N. Yu et al. [135] evaluated DKI values in lymph node involvement (85 patients with 273 lymph nodes). Dapp, Kapp, and ADC of the lymph nodes were evaluated. Median Dapp and ADC values of malignant lymph nodes were significantly higher than in benign lymph nodes, while median Kapp of malignant lymph nodes was statistically lower than in normal lymph nodes [135].

Yu et al. [136] assessed the correlation between DWI and DKI and distant metastases showing that the Dapp was significantly lower in patients with metastases [136].

Regarding the response to treatment in LARC, Yu et al. [137] evaluated DKI as a biomarker to predict the response in LARC. Researchers demonstrated that percentage change in Dapp has higher diagnostic performance for assessing response to treatment. Hu et al. [138] evaluated DKI parameters as biomarkers of complete response relative to ADC, demonstrating that MKpre and MKpost values were much lower for responder patients than for non-responders, while ADCpost and rate of change ADCs were significantly higher for responder patients. Fusco et al. [123] evaluated the tumor response to short-term radiotherapy using the standardized index of shape (SIS) by contrast magnetic resonance imaging,

ADC, IVIM and DKI parameters. Promising results were obtained using a decision tree tested with all ADC, IVIM and DKI parameters.

DKI is a promising approach in evaluating LARC patients; however, the DKI must be a reproducible model. Therefore, to obtain quantitative parameters it is necessary to standardize the sequence and the model [139, 140].

Renal tumours

Renal cell carcinoma (RCC) is the most frequent malignant renal tumour in adults and surgical resection is the main valuable approach; other options, comprising RFA, cytoablation and even active surveillance have been employed [141–151]. In patients unfit for surgery, systemic therapy including targeted agents, immunotherapy and chemotherapy were employed to improve the overall survival (OS) [141–151]. In this context, lesion detection and identification of histologic grades has clinical significance in establishing prognosis.

Ding et al. [152] showed that DKI was a feasible tool in characterization of malignant lesions, with the MD higher, while MK lower than those of benign lesions [152]. In addition, Fu et al. [153] assessed the DKI in RCC, considering 66 patients, 13 with renal angiomyolipoma with minimal fat (RAMF) and 7 patients with renal oncocytoma (RO). MD, fractional Anisotropy (FA), MK, kurtosis anisotropy (KA) and radial kurtosis (RK) were calculated. For MD, a significant higher value was shown in RCC than the rest renal tumors. The MD values were higher for RO than for AML, while comparable MD values were found between RCC and RO. For MK, KA and RK, a significant higher value was demonstrated in AML than RCC and RO. The MK, KA and RK values were higher for RO than for RCC [153]. Zhu et al. [154] assessed the feasibility and reproducibility of diffusion kurtosis tensor imaging (DKTI) in RCC in distinguishing the subtypes of RCC and the grades of clear cell RCC (CCRCC). They found significant differences between the DKTI metrics of RCCs and contralateral renal parenchyma among the subtypes of RCC. MK and Ka values of CRCC were significantly higher than those of CCRCC and contralateral normal parenchyma (PRCC). Statistical difference of the MK, KA, RK and MD values were also obtained between CCRCC with high- and low-grades. MK values were more effective for distinguishing between low- and high- grade. These data were similar to ones of Cao et al. [155] that analysed 89 patients with histologically proven ccRCC, showing that compared to normal renal parenchyma, ADC and MD values of ccRCC decreased and MK, Ka, and Kr values increased. ADC and MD values of ccRCC decreased with the increase in pathological grade, while MK, Ka, and Kr

values were increased. ADC could discriminate the grading except for G1 versus G2 while Ka and Kr the grading except for G2 versus G3 and MD and MK could discriminate G1 versus G2, G1 versus G3, G1 versus G4, G2 versus G3, G2 versus G4, and G3 versus G4. The AUC of MK was the highest [155].

Although several researches have demonstrated the potential role of DKI in the assessment of several prognostic features and, so to guide a precise treatment, however the potential advantage of using DKI in the kidneys remains to be fully explored.

Prostate cancer

In the last decade, there has been growing attention on MRI of the prostate as new imaging tool, that thanks to the association of DWI and DCE with conventional T1- and T2-W imaging, now it is possible to obtain a multiparametric MRI (mpMRI) protocols [28, 30, 156–163].

Several researches have assessed DKI and DWI in the assessment of tumour aggressiveness (Fig. 4). However, the results have been contradictory: several studies demonstrated a better performance of DKI [164, 165], others did not prove these data [166–168]. Rosenkrantz et al. [164] showed that K values were significantly higher in both tumor than normal parenchyma and tumor with higher rather than lower Gleason scores. Furthermore, DKI showed significantly greater sensitivity than ADC to differentiate cancerous areas from benign areas in the peripheral zone (PZ). Roethke et al. [167], evaluating 55 patients with prostate cancer, did not confirm these results, showing that although K was significantly higher in areas with cancer, the ROC analysis did not show a significant difference between DKI and ADC to detect the cancer. As for the aggression, Kapp and ADC showed a comparable result.

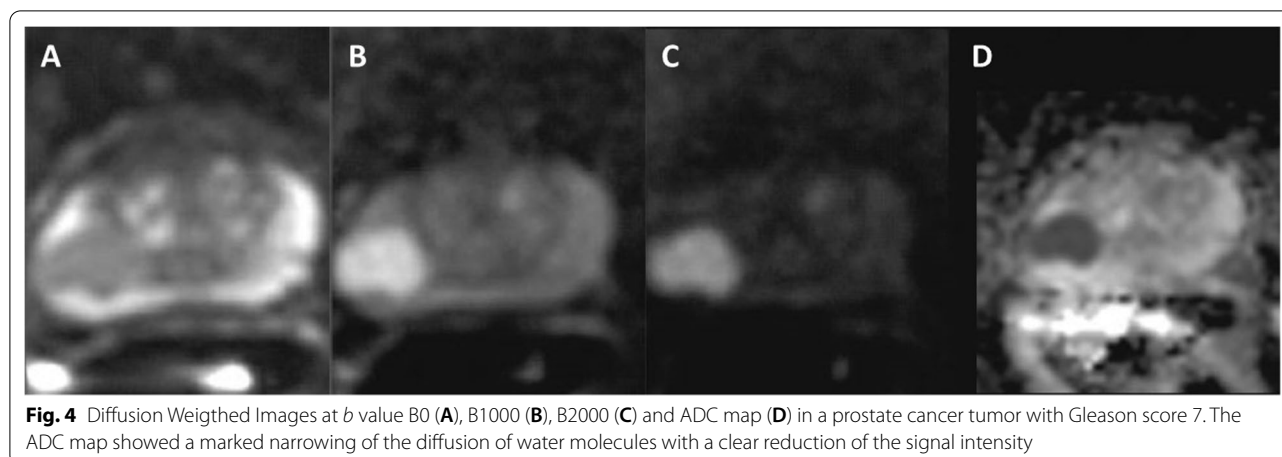
A recent study comparing ADC and DKI in detection and characterization, evaluating 255 patients with PC [169]. The authors showed that ADC and DKI had a similar diagnostic performance, so that they concluded that there was not a clear benefit of DKI.

Therefore, the value of additional DKI remains unclear. Anyway, the present data propose that DKI could offer different but complementary information on tumour microenvironment.

Other fields

Few studies have evaluated the role of DKI in cervical or endometrial cancer [170–172].

Cervical cancer (UCC) was the fourth most commonly diagnosed malignancy and the fourth leading cause of cancer death among women worldwide [13, 173–178]. Cervical squamous carcinoma (CSC) is the most common pathological type of UCC, accounting for 75–80% of



the total number of cervical cancer patients [170]. Poorly differentiated CSCs can easily cause local invasion and distant metastasis, influencing the choice of treatment and patient prognosis. Therefore, it is important to accurately assess the degree of CSC before treatment. Hou et al. compared the weighted imaging value for amide proton transfer (APTWI) and DKI in evaluating the histological grade of cervical squamous carcinoma (CSC) in addition to DWI [170]. They showed that the APTWI (MTRasym) parameters and MK values of G1 were significantly lower than those of G2 and those parameters of G2 were significantly lower than those of G3. The MD and ADC values of G1 were significantly higher than those of G2 and those of G2 were significantly higher than those of G3. MTRasym and MK were both positively correlated with histological grade, while MD and ADC were both negatively correlated with histological grade.

Endometrial cancer (EC) is the most common gynecological malignancy in the world. Prognosis depends on several factors, including histological grade and subtype, International Federation of Gynecology and Obstetrics (FIGO) stage, lymphovascular invasion, and lymph node metastases. The histological grade of endometrial cancer alone is a strong predictor of lymph node metastasis [130, 178–182]. Although several studies have explored the value of whole tumor histogram analysis of ADC for preoperative tumor classification of endometrial cancer, few studies have evaluated the value of DKI. Chen et al. [171] evaluated 73 patients with CE and compared Dapp, Kapp and ADC parameters between high-grade (grade 3) and low-grade (grade 1 and 2) tumors, demonstrating that the 10th percentile AUC Dapp, Kapp's 90th percentile, and ADC The 10th percentile was superior to other parameters in distinguishing high-grade from low-grade cancers. The combination of the 10th percentile of Dapp

and the 90th percentile of Kapp improved the AUC to 0.901, which was significantly higher than that of the 10th percentile of the ADC.

Yue et al. [172] compared the performance of DKI and DWI for diagnosis and histological classification of EC. They evaluated 61 EC patients and 30 patients with normal endometrium; showed that MK values for groups G0, G1, G2 and G3 gradually increased, while MD and ADC values gradually decreased. MK values had the highest diagnostic accuracy in differentiating G0 and (G1 + G2 + G3), G0 and G1, G1 and G2 and G2 and G3. MK was maximally correlated with histological grade, followed by MD and ADC [172].

Discussion and conclusion

DKI provides more data on tissue structures than the conventional monoexponential model for b -values below 1000 s/mm^2 . Advances in hardware and software within modern MRI scanners now allow for ultra-high b -value imaging, hence the ability to apply DKI to multiple extracranial sites. Therefore, body radiologists could benefit from a better understanding of the main concepts of DKI.

Several studies have evaluated the ability of DKI in tumor characterization and tumor grade assessment. DKI parameters could help distinguish benign from malignant tissues, as several research suggests that DKI parameters outperform ADC to distinguish low- and high-grade lesions. However, these researches observe an inverse association between Kapp and ADC, raising the question of whether there is an additional advantage of DKI, given the increased technical complexity.

Additionally, in several studies the DKI sequences used were based on planar echo (EPI) acquisition, which is susceptible to motion, metal and air artefacts and prone to low SNRs and distortions, leading to low

quality images for some small lesions, which may affect the accuracy of the results. Another problem is the optimal *b*-value of DKI, which remains to be explored since a publicly recognized standard has not yet been introduced, as well as the manually selected region of interest, which could affect the accuracy of some parameters.

In conclusion, DKI is still largely a research tool and few data support its routine use compared to conventional DWI in oncology. However, the technique is at a stage where it can be explored in broader clinical settings.

Abbreviations

DWI: Diffusion-weighted imaging; MRI: Magnetic resonance imaging; SI: Signal intensity; ADC: Apparent diffusion coefficient; DKI: Diffusion kurtosis imaging; MK: Kurtosis median coefficient; MD: Mean diffusion coefficient; SNR: Signal-to-noise ratio; HCC: Hepatocellular carcinoma; MVI: Microvascular invasion; STD: Standard deviation; FP: Perfusion fraction; AUC: Area under curve; IVIM: Intravoxel incoherent motion; PDACs: Pancreatic ductal adenocarcinomas; PNETs: Pancreatic neuroendocrine tumors; SPNs: Solid pseudo papillary neoplasms; ECT: Electrochemotherapy; RECIST: Response evaluation criteria in solid tumour; LARC: Locally advanced rectal cancer; pCRT: Preoperative chemoradiotherapy; LVI: Lymphovascular invasion; CRM: Circumferential margin; SIS: Standardized index of shape; RCC: Renal cell carcinoma; RFA: Radiofrequency ablation; OS: Overall survival; RAMF: Renal angiomyolipoma with minimal fat; RO: Renal oncocytoma; FA: Fractional anisotropy; KA: Kurtosis anisotropy; RK: Radial kurtosis; AML: Renal angiomyolipoma; DKI: Diffusion kurtosis tensor imaging; CCRCC: Clear cell RCC; PRCC: Contralateral normal parenchyma; DCE: Dynamic contrast enhanced; mpMRI: Multiparametric MRI; UCC: Cervical cancer; CSC: Cervical squamous carcinoma; APTWI: Weighted imaging value for amide proton transfer; EC: Endometrial cancer; FIGO: International federation of gynecology and obstetrics; EPI: Echo planar imaging.

Acknowledgements

The authors are grateful to Alessandra Trocino, librarian at the National Cancer Institute of Naples, Italy. Moreover, for their collaboration, the authors are grateful for the research support of Paolo Pariante, Martina Totaro and Andrea Esposito of Radiology Division, "Istituto Nazionale Tumori IRCCS Fondazione Pascale—IRCCS di Napoli", Naples, I-80131, Italy.

Author contributions

Conceptualization, VG; Investigation, VG, AB, GD, EB, CC, AP, FI; VG wrote and revised the manuscript. Each author has participated sufficiently to take public responsibility for the content of the manuscript. All authors read and approved the final manuscript.

Funding

No funding.

Availability of data and materials

Data are available at <https://zenodo.org/record/6598327#.YpX2A2hBy3A>.

Declarations

Ethics approval and consent to participate

Not applicable.

Consent for publication

Not applicable.

Competing interests

The authors that they have no competing interests.

Author details

¹Division of Radiology, "Istituto Nazionale Tumori IRCCS Fondazione Pascale—IRCCS di Napoli", I-80131 Naples, Italy. ²Medical Oncology Division, Igea Spa, Naples, Italy. ³Division of Hepatobiliary Surgical Oncology, "Istituto Nazionale Tumori IRCCS Fondazione Pascale—IRCCS di Napoli", I-80131 Naples, Italy. ⁴Department of Radiology, Azienda Ospedaliero-Universitaria Careggi, Florence, Italy. ⁵Italian Society of Medical and Interventional Radiology, SIRM Foundation, Milan, Italy. ⁶Department of Medicine, Surgery and Dentistry, University of Salerno, Salerno, Italy.

Received: 30 April 2022 Accepted: 30 May 2022

Published online: 09 June 2022

References

- Granata V, Grassi R, Fusco R, Belli A, Cutolo C, Pradella S, Grazzini G, La Porta M, Brunese MC, De Muzio F, Ottaiano A, Avallone A, Izzo F, Petrillo A. Diagnostic evaluation and ablation treatments assessment in hepatocellular carcinoma. *Infect Agent Cancer*. 2021;16(1):53. <https://doi.org/10.1186/s13027-021-00393-0>.
- Barabino M, Gurgitano M, Fochesato C, Angileri SA, Franceschelli G, Santambrogio R, Mariani NM, Opocher E, Carrafiello G. LI-RADS to categorize liver nodules in patients at risk of HCC: Tool or a gadget in daily practice? *Radiol Med*. 2021;126(1):5–13. <https://doi.org/10.1007/s11547-020-01225-8>.
- Gabelloni M, Di Nasso M, Morganti R, Faggioni L, Masi G, Falcone A, Neri E. Application of the ESR iGuide clinical decision support system to the imaging pathway of patients with hepatocellular carcinoma and cholangiocarcinoma: preliminary findings. *Radiol Med*. 2020;125(6):531–7. <https://doi.org/10.1007/s11547-020-01142-w>.
- Granata V, Grassi R, Fusco R, Setola SV, Belli A, Ottaiano A, Nasti G, La Porta M, Danti G, Cappabianca S, Cutolo C, Petrillo A, Izzo F. Intrahepatic cholangiocarcinoma and its differential diagnosis at MRI: how radiologist should assess MR features. *Radiol Med*. 2021;126(12):1584–600. <https://doi.org/10.1007/s11547-021-01428-7>.
- Granata V, Bicchierai G, Fusco R, Cozzi D, Grazzini G, Danti G, De Muzio F, Maggialelli N, Smorchkova O, D'Elia M, Brunese MC, Grassi R, Giacobbe G, Bruno F, Palumbo P, Grassi F, Brunese L, Grassi R, Miele V, Barile A. Diagnostic protocols in oncology: workup and treatment planning. Part 2: abbreviated MR protocol. *Eur Rev Med Pharmacol Sci*. 2021;25(21):6499–528. https://doi.org/10.26355/eurrev_202111_27094.
- Granata V, Fusco R, Amato DM, Albino V, Patrone R, Izzo F, Petrillo A. Beyond the vascular profile: conventional DWI, IVIM and kurtosis in the assessment of hepatocellular carcinoma. *Eur Rev Med Pharmacol Sci*. 2020;24(13):7284–93. https://doi.org/10.26355/eurrev_202007_21883.
- Granata V, Fusco R, Maio F, Avallone A, Nasti G, Palaia R, Albino V, Grassi R, Izzo F, Petrillo A. Qualitative assessment of EOB-GD-DTPA and Gd-BT-DO3A MR contrast studies in HCC patients and colorectal liver metastases. *Infect Agent Cancer*. 2019;27(14):40. <https://doi.org/10.1186/s13027-019-0264-3>.
- Gatti M, Calandri M, Bergamasco L, Darvizeh F, Grazioli L, Inchingolo R, Ippolito D, Rousset S, Veltri A, Fonio P, Faletti R. Characterization of the arterial enhancement pattern of focal liver lesions by multiple arterial phase magnetic resonance imaging: comparison between hepatocellular carcinoma and focal nodular hyperplasia. *Radiol Med*. 2020;125(4):348–55. <https://doi.org/10.1007/s11547-019-01127-7>.
- Granata V, Fusco R, Avallone A, Catalano O, Filice F, Leongito M, Palaia R, Izzo F, Petrillo A. Major and ancillary magnetic resonance features of LI-RADS to assess HCC: an overview and update. *Infect Agent Cancer*. 2017;28(12):23. <https://doi.org/10.1186/s13027-017-0132-y>.
- Granata V, Fusco R, Avallone A, Filice F, Tatangelo F, Piccirillo M, Grassi R, Izzo F, Petrillo A. Critical analysis of the major and ancillary imaging features of LI-RADS on 127 proven HCCs evaluated with functional and morphological MRI: lights and shadows. *Oncotarget*. 2017;8(31):51224–37. <https://doi.org/10.18632/oncotarget.17227>.
- Granata V, Grassi R, Fusco R, Setola SV, Palaia R, Belli A, Miele V, Brunese L, Grassi R, Petrillo A, Izzo F. Assessment of ablation therapy in pancreatic cancer: the radiologist's challenge. *Front Oncol*. 2020;27(10):560952. <https://doi.org/10.3389/fonc.2020.560952>.

12. Granata V, Fusco R, Catalano O, Piccirillo M, De Bellis M, Izzo F, Petrillo A. Percutaneous ablation therapy of hepatocellular carcinoma with irreversible electroporation: MRI findings. *AJR Am J Roentgenol*. 2015;204(5):1000–7. <https://doi.org/10.2214/AJR.14.12509>.
13. Gurgitano M, Angileri SA, Rodà GM, Liguori A, Pandolfi M, Ierardi AM, Wood BJ, Carrafiello G. Interventional radiology ex-machina: impact of artificial intelligence on practice. *Radiol Med*. 2021;126(7):998–1006. <https://doi.org/10.1007/s11547-021-01351-x>.
14. Brizi MG, Perillo F, Cannone F, Tuzza L, Manfredi R. The role of imaging in acute pancreatitis. *Radiol Med*. 2021;126(8):1017–29. <https://doi.org/10.1007/s11547-021-01359-3>.
15. Assadsangabi R, Babaei R, Songco C, Ivanovic V, Bobinski M, Chen YJ, Nabavizadeh SA. Multimodality oncologic evaluation of superficial neck and facial lymph nodes. *Radiol Med*. 2021;126(8):1074–84. <https://doi.org/10.1007/s11547-021-01367-3>.
16. Mathew RP, Sam M, Raubenheimer M, Patel V, Low G. Hepatic hemangiomas: the various imaging avatars and its mimickers. *Radiol Med*. 2020;125(9):801–15. <https://doi.org/10.1007/s11547-020-01185-z>.
17. Granata V, Fusco R, Avallone A, De Stefano A, Ottaiano A, Sbordone C, Brunese L, Izzo F, Petrillo A. Radiomics-derived data by contrast enhanced magnetic resonance in RAS mutations detection in colorectal liver metastases. *Cancers (Basel)*. 2021;13(3):453. <https://doi.org/10.3390/cancers13030453>.
18. Esposito A, Buscarino V, Raciti D, Casiraghi E, Manini M, Biondetti P, Forzenigo L. Characterization of liver nodules in patients with chronic liver disease by MRI: performance of the liver imaging reporting and data system (LI-RADS vol 2018) scale and its comparison with the likert scale. *Radiol Med*. 2020;125(1):15–23. <https://doi.org/10.1007/s11547-019-01092-y>.
19. Granata V, Fusco R, Filice S, Catalano O, Piccirillo M, Palaia R, Izzo F, Petrillo A. The current role and future perspectives of functional parameters by diffusion weighted imaging in the assessment of histologic grade of HCC. *Infect Agent Cancer*. 2018;3(13):23. <https://doi.org/10.1186/s13027-018-0194-5>.
20. Orlacchio A, Chegaf F, Roma S, Merolla S, Bosa A, Francioso S. Degradable starch microspheres transarterial chemoembolization (DSMs-TACE) in patients with unresectable hepatocellular carcinoma (HCC): long-term results from a single-center 137-patient cohort prospective study. *Radiol Med*. 2020;125(1):98–106. <https://doi.org/10.1007/s11547-019-01093-x>.
21. Granata V, Fusco R, Filice S, Incollingo P, Belli A, Izzo F, Petrillo A. Comment on “state of the art in magnetic resonance imaging of hepatocellular carcinoma”: the role of DWI. *Radiol Oncol*. 2019;53(3):369–70. <https://doi.org/10.2478/raon-2019-0031>.
22. Bozkurt M, Eldem G, Bozbulut UB, Bozkurt MF, Kılıçkap S, Peynircioğlu B, Çil B, Lay Ergün E, Volkan-Salancı B. Factors affecting the response to Y-90 microsphere therapy in the cholangiocarcinoma patients. *Radiol Med*. 2021;126(2):323–33. <https://doi.org/10.1007/s11547-020-01240-9>.
23. Kim BH, Kim JS, Kim KH, Moon HJ, Kim S. Clinical significance of radiation dose-volume parameters and functional status on the patient-reported quality of life changes after thoracic radiotherapy for lung cancer: a prospective study. *Radiol Med*. 2021;126(3):466–73. <https://doi.org/10.1007/s11547-020-01273-0>.
24. Orsatti G, Zucchetto P, Varotto A, Crimi F, Weber M, Cecchin D, Bisogno G, Spimpolo A, Giraudo C, Stramare R. Volumetric histograms-based analysis of apparent diffusion coefficients and standard uptake values for the assessment of pediatric sarcoma at staging: preliminary results of a PET/MRI study. *Radiol Med*. 2021. <https://doi.org/10.1007/s11547-021-01340-0>.
25. Jensen JH, Helpert J. MRI quantification of non-gaussian water diffusion by kurtosis analysis. *NMR Biomed*. 2010;23(7):698–710. <https://doi.org/10.1002/nbm.1518>.
26. Trombadori CML, D'Angelo A, Ferrara F, Santoro A, Belli P, Manfredi R. Radial scar: a management dilemma. *Radiol Med*. 2021. <https://doi.org/10.1007/s11547-021-01344-w>.
27. Rosenkrantz AB, Padhani AR, Chenevert TL, Koh DM, De Keyzer F, Taouli B, Le Bihan D. Body diffusion kurtosis imaging: basic principles, applications, and considerations for clinical practice. *J Magn Reson Imaging*. 2015;42(5):1190–202. <https://doi.org/10.1002/jmri.24985>.
28. Scialpi M, Scialpi P, Martorana E, Torre R, Manciola FA, D'Andrea A, Di Blasi A. Biparametric MRI with simplified PI-RADS (S-PI-RADS) for prostate cancer detection and management: what do radiologist need to know. *Radiol Med*. 2021;126(12):1660–1. <https://doi.org/10.1007/s11547-021-01343-x>.
29. Cellina M, Gibelli D, Martinenghi C, Giardini D, Soresina M, Menozzi A, Oliva G, Carrafiello G. Non-contrast magnetic resonance lymphography (NCMLR) in cancer-related secondary lymphedema: acquisition technique and imaging findings. *Radiol Med*. 2021;126(11):1477–86. <https://doi.org/10.1007/s11547-021-01410-3>.
30. Chen C, Yang Z, Sweeney E, Hectors SJ, Hu JC, Margolis DJ. Prostate heterogeneity correlates with clinical features on multiparametric MRI. *Abdom Radiol (NY)*. 2021;46(11):5369–76. <https://doi.org/10.1007/s00261-021-03221-6>.
31. Mazzola R, Cuccia F, Figlia V, Rigo M, Nicosia L, Gajj-Levra N, Ricchetti F, Vitale C, Mantoan B, Di Paola G, De Simone A, Gurrera D, Sicignano G, Naccarato S, Ruggieri R, Alongi F. Stereotactic body radiotherapy for oligometastatic castration sensitive prostate cancer using 1.5 T MRI-Linac: preliminary data on feasibility and acute patient-reported outcomes. *Radiol Med*. 2021;126(7):989–97. <https://doi.org/10.1007/s11547-021-01352-w>.
32. Arita Y, Yoshida S, Waseda Y, Takahara T, Ishii C, Ueda R, Kwee TC, Miyahira K, Ishii R, Okuda S, Jinzaki M, Fujii Y. Diagnostic value of computed high b-value whole-body diffusion-weighted imaging for primary prostate cancer. *Eur J Radiol*. 2021;137:109581. <https://doi.org/10.1016/j.ejrad.2021.109581>.
33. Santone A, Brunese MC, Donnarumma F, Guerriero P, Mercedo F, Reginelli A, Miele V, Giovagnoni A, Brunese L. Radiomic features for prostate cancer grade detection through formal verification. *Radiol Med*. 2021;126(5):688–97. <https://doi.org/10.1007/s11547-020-01314-8>.
34. Fersino S, Borghesi S, Jereczek-Fossa BA, Arcangeli S, Mortellaro G, Magrini SM, Alongi F. Uro-Oncology study group of Italian association of radiotherapy and clinical oncology (AIRO). PROACTA: a survey on the actual attitude of the Italian radiation oncologists in the management and prescription of hormonal therapy in prostate cancer patients. *Radiol Med*. 2021;126(3):460–5. <https://doi.org/10.1007/s11547-020-01264-1>.
35. Klingebiel M, Ullrich T, Quentin M, Bonekamp D, Aissa J, Mally D, Arsov C, Albers P, Antoch G, Schimmöller L. Advanced diffusion weighted imaging of the prostate: Comparison of readout-segmented multi-shot, parallel-transmit and single-shot echo-planar imaging. *Eur J Radiol*. 2020;130:109161. <https://doi.org/10.1016/j.ejrad.2020.109161>.
36. Kusunoki M, Kikuchi K, Togao O, Yamashita K, Momosaka D, Kikuchi Y, Kuga D, Hata N, Mizoguchi M, Iihara K, Suzuki SO, Iwaki T, Akamine Y, Hiwatashi A. Differentiation of high-grade from low-grade diffuse gliomas using diffusion-weighted imaging: a comparative study of mono-, bi-, and stretched-exponential diffusion models. *Neuroradiology*. 2020;62(7):815–23. <https://doi.org/10.1007/s00234-020-02456-2>.
37. Taoka T, Naganawa S, Kawai H, Nakane T, Murata K. Can low b value diffusion weighted imaging evaluate the character of cerebrospinal fluid dynamics? *Jpn J Radiol*. 2019;37(2):135–44. <https://doi.org/10.1007/s11604-018-0790-8>.
38. Di Giuliano F, Minosse S, Picchi E, Ferrazzoli V, Da Ros V, Muto M, Pistolesi CA, Garaci F, Floris R. Qualitative and quantitative analysis of 3D T1 silent imaging. *Radiol Med*. 2021;126(9):1207–15. <https://doi.org/10.1007/s11547-021-01380-6>.
39. Detti B, Scoccianti S, Teriaca MA, Maragna V, Lorenzetti V, Lucidi S, Bellini C, Greto D, Desideri I, Livi L. Bevacizumab in recurrent high-grade glioma: a single institution retrospective analysis on 92 patients. *Radiol Med*. 2021;126(9):1249–54. <https://doi.org/10.1007/s11547-021-01381-5>.
40. Romano N, Castaldi A. Imaging of intracranial fat: from normal findings to pathology. *Radiol Med*. 2021;126(7):971–8. <https://doi.org/10.1007/s11547-021-01365-5>.
41. Paoletti M, Muzic SJ, Marchetti F, Farina LM, Bastianello S, Pichiechio A. Differential imaging of atypical demyelinating lesions of the central nervous system. *Radiol Med*. 2021;126(6):827–42. <https://doi.org/10.1007/s11547-021-01334-y>.
42. Liheng M, Guofan X, Balzano RF, Yuying L, Weifeng H, Ning Y, Yayun J, Mouyuan L, Guglielmi G. The value of DTI: achieving high diagnostic performance for brain metastasis. *Radiol Med*. 2021;126(2):291–8. <https://doi.org/10.1007/s11547-020-01243-6>.

43. Jiang W, Zhao Z, Wu Q, Wang L, Zhou L, Li D, He L, Tan Y. Study on brain structure network of patients with delayed encephalopathy after carbon monoxide poisoning: based on diffusion tensor imaging. *Radiol Med.* 2021;126(1):133–41. <https://doi.org/10.1007/s11547-020-01222-x>.
44. Gunbey HP, Has AC, Aslan K, Saglam D, Avci U, Sayit AT, Incesu L. Microstructural white matter abnormalities in hypothyroidism evaluation with diffusion tensor imaging tract-based spatial statistical analysis. *Radiol Med.* 2021;126(2):283–90. <https://doi.org/10.1007/s11547-020-01234-7>.
45. Shin N, Choi JA, Choi JM, Cho ES, Kim JH, Chung JJ, Yu JS. Sclerotic changes of cavernous hemangioma in the cirrhotic liver: long-term follow-up using dynamic contrast-enhanced computed tomography. *Radiol Med.* 2020;125:1225–32.
46. Pietragalla M, Nardi C, Bonasera L, Mungai F, Verrone GB, Calistri L, Taverna C, Novelli L, Lo-cattello LG, Mannelli G, Gallo O, Miele V. Current role of computed tomography imaging in the evaluation of cartilage invasion by laryngeal carcinoma. *Radiol Med.* 2020;125:1301–10.
47. Gentili F, Bronico I, Maestroni U, Ziglioli F, Silini EM, Buti S, de Filippo M. Small renal masses (≤ 4 cm): differentiation of oncocytoma from renal clear cell carcinoma using ratio of lesion to cortex attenuation and aorta-lesion attenuation difference (ALAD) on contrast-enhanced CT. *Radiol Med.* 2020;125:1280–7.
48. Granata V, Grassi R, Fusco R, Galdiero R, Setola SV, Palaia R, Belli A, Silvestro L, Cozzi D, Brunese L, Petrillo A, Izzo F. Pancreatic cancer detection and characterization: state of the art and radiomics. *Eur Rev Med Pharmacol Sci.* 2021;25:3684–99.
49. Fusco R, Granata V, Pariante P, Cerciello V, Siani C, Di Bonito M, Valentino M, Sansone M, Botti G, Petrillo A. Blood oxygenation level dependent magnetic resonance imaging and diffusion weighted MRI imaging for benign and malignant breast cancer discrimination. *Magn Reson Imaging.* 2021;75:51–9.
50. Esposito A, Gallone G, Palmisano A, Marchitelli L, Catapano F, Francone M. The current landscape of imaging recommendations in cardiovascular clinical guidelines: toward an imaging-guided precision medicine. *Radiol Med.* 2020;125:1013–23.
51. Albano D, Stecco A, Micci G, Sconfienza LM, Colagrande S, Reginelli A, Grassi R, Carriero A, Midiri M, Lagalla R, Galia M. Whole-body magnetic resonance imaging (WB-MRI) in oncology: an Italian survey. *Radiol Med.* 2021;126:299–305.
52. Fusco R, Granata V, Petrillo A. Introduction to special issue of radiology and imaging of cancer. *Cancers (Basel).* 2020;12:2665.
53. Zhang A, Song J, Ma Z, Chen T. Combined dynamic contrast-enhanced magnetic resonance imaging and diffusion-weighted imaging to predict neoadjuvant chemotherapy effect in FIGO stage IB2-IIA2 cervical cancers. *Radiol Med.* 2020;125:1233–42.
54. Gentili F, Bronico I, Maestroni U, Ziglioli F, Silini EM, Buti S, de Filippo M. Small renal masses (≤ 4 cm): differentiation of oncocytoma from renal clear cell carcinoma using ratio of lesion to cortex attenuation and aorta-lesion attenuation difference (ALAD) on contrast-enhanced CT. *Radiol Med.* 2020;125:1280–7.
55. Pediconi F, Galati F, Bernardi D, Belli P, Brancato B, Calabrese M, Camera L, Carbonaro LA, Caumo F, Clauser P, Girardi V, Iaconi C, Martincich L, Panizza P, Petrillo A, Schiaffino S, Tagliafico A, Trimboli RM, Zuiani C, Sardaneli F, Montemezzi S. Breast imaging and cancer diagnosis during the COVID-19 pandemic: recommendations from the Italian college of breast radiologists by SIRM. *Radiol Med.* 2020;125:926–30.
56. Petralia G, Summers PE, Agostini A, Ambrosini R, Cianci R, Cristel G, Calistri L, Colagrande S. Dynamic contrast-enhanced MRI in oncology: how we do it. *Radiol Med.* 2020;125:1288–300.
57. Crimi F, Capelli G, Spolverato G, Bao QR, Florio A, Milite Rossi S, Cecchin D, Albertoni L, Campi C, Pucciarelli S, Stramare R. MRI T2-weighted sequences-based texture analysis (TA) as a predictor of response to neoadjuvant chemo-radiotherapy (nCRT) in patients with locally advanced rectal cancer (LARC). *Radiol Med.* 2020;125:1216–24.
58. Gaia C, Maria Chiara C, Silvia L, Chiara A, Maria Luisa C, Giulia B, Silvia P, Lucia C, Alessandra T, Annarita S, Cristina V, Maria A, Maria Rosaria D, Giacinta A, Riccardo G, Zaher K, Andrea L, Maddalena B, Catalano C, Paolo R. Chest CT for early detection and management of coronavirus disease (COVID-19): a report of 314 patients admitted to emergency department with suspected pneumonia. *Radiol Med.* 2020;125:931–42.
59. Aberle S, Kenkel D, Becker AS, Puipe G, Burger I, Schaefer N, Pfammatter T. Outpatient Yttrium-90 microsphere radioembolization: assessment of radiation safety and quantification of post-treatment adverse events causing hospitalization. *Radiol Med.* 2020;125:971–80.
60. Danti G, Berti V, Abenavoli E, Briganti V, Linguanti F, Mungai F, Pradella S, Miele V. Diagnostic imaging of typical lung carcinoids: relationship between MDCT, 111In-Octreoscan and 18F-FDG-PET imaging features with Ki-67 index. *Radiol Med.* 2020;125:715–29.
61. Zhang G, Yang Z, Gong L, Jiang S, Wang L, Zhang H. Classification of lung nodules based on CT images using squeeze-and-excitation network and aggregated residual transformations. *Radiol Med.* 2020;125:374–83.
62. Granata V, Grassi R, Fusco R, Belli A, Palaia R, Carrafiello G, Miele V, Grassi R, Petrillo A, Izzo F. Local ablation of pancreatic tumors: state of the art and future perspectives. *World J Gastroenterol.* 2021;27:3413–28.
63. Granata V, Fusco R, Salati S, Petrillo A, Di Bernardo E, Grassi R, Palaia R, Danti G, La Porta M, Cadossi M, Gašljević G, Sersa G, Izzo F. A systematic review about imaging and histopathological findings for detecting and evaluating electroporation based treatments response. *Int J Environ Res Public Health.* 2021;18:5592.
64. Fusco R, Granata V, Sansone M, Rega D, Delrio P, Tatangelo F, Romano C, Avallone A, Pupo D, Giordano M, Grassi R, Ravo V, Pecori B, Petrillo A. Validation of the standardized index of shape tool to analyze DCE-MRI data in the assessment of neo-adjuvant therapy in locally advanced rectal cancer. *Radiol Med.* 2021;126:1044–54.
65. Granata V, Fusco R, de Lutio di Castelguidone E, Avallone A, Palaia R, Delrio P, Tatangelo F, Botti G, Grassi R, Izzo F, Petrillo A. Diagnostic performance of gadoteric acid-enhanced liver MRI versus multidetector CT in the assessment of colorectal liver metastases compared to hepatic resection. *BMC Gastroenterol.* 2019;19:129.
66. Granata V, Fusco R, Amato DM, Albino V, Patrone R, Izzo F, Petrillo A. Beyond the vascular profile: conventional DWI, IVIM and kurtosis in the assessment of hepatocellular carcinoma. *Eur Rev Med Pharmacol Sci.* 2020;24:7284–93.
67. Bi Y, Zhu X, Yu Z, Jiao D, Yi M, Han X, Ren J. Radioactive feeding tube in the palliation of esophageal malignant obstruction. *Radiol Med.* 2020;125:544–50.
68. Hu HT, Shan QY, Chen SL, Li B, Feng ST, Xu EJ, Li X, Long JY, Xie XY, Lu MD, Kuang M, Shen JX, Wang W. CT-based radiomics for pre-operative prediction of early recurrent hepatocellular carcinoma: technical reproducibility of acquisition and scanners. *Radiol Med.* 2020;125:697–705.
69. Mathew RP, Sam M, Raubenheimer M, Patel V, Low G. Hepatic hemangiomas: the various imaging avatars and its mimickers. *Radiol Med.* 2020;125:801–15.
70. Franceschini D, Bruni A, Borghetti P, Gaj-Levra N, Ramella S, Buffoni L, Badellino S, Andolina M, Comin C, Vattemi E, Bezzi M, Trovò M, Passaro A, Bearz A, Chiari R, Tindara F, Ferrari K, Piperno F, Filippi AR, Novovesi D, Scotti V. Is multidisciplinary management possible in the treatment of lung cancer? A report from three Italian meetings. *Radiol Med.* 2020;125:214–9.
71. Shlomi D, Ben-Avi R, Balmor GR, Onn A, Peled N. Screening for lung cancer: time for large-scale screening by chest computed tomography. *Eur Respir J.* 2014;44:217–38.
72. Granata V, Fusco R, Costa M, Picone C, Cozzi D, Moroni C, La Casella GV, Montanino A, Monti R, Mazzoni F, Grassi R, Malagnino VG, Cappabianca S, Grassi R, Miele V, Petrillo A. Preliminary report on computed tomography radiomics features as biomarkers to immunotherapy selection in lung adenocarcinoma patients. *Cancers.* 2021;13:3992.
73. De Filippo M, Ziglioli F, Russo U, Pagano P, Brunese L, Bertelli E, Pagnini F, Maestroni U. Radiofrequency ablation (RFA) of T1a renal cancer with externally cooled multitined expandable electrodes. *Radiol Med.* 2020;125(8):790–7. <https://doi.org/10.1007/s11547-020-01175-1>.
74. Arrigoni F, Bruno F, Gianneramo C, Palumbo P, Zugaro L, Zoccali C, Barile A, Masciocchi C. Evolution of the imaging features of osteoid osteoma treated with RFA or MRgFUS during a long-term follow-up: a pictorial review with clinical correlations. *Radiol Med.* 2020;125(6):578–84. <https://doi.org/10.1007/s11547-020-01134-w>.
75. Granata V, Fusco R, Setola SV, Avallone A, Palaia R, Grassi R, Izzo F, Petrillo A. Radiological assessment of secondary biliary tree lesions: an update.

- J Int Med Res. 2020;48(6):300060519850398. <https://doi.org/10.1177/0300060519850398>.
76. Granata V, Fusco R, Catalano O, Avallone A, Palaia R, Botti G, Tatangelo F, Granata F, Cascella M, Izzo F, Petrillo A. Diagnostic accuracy of magnetic resonance, computed tomography and contrast enhanced ultrasound in radiological multimodality assessment of peribiliary liver metastases. *PLoS ONE*. 2017;12(6):e0179951. <https://doi.org/10.1371/journal.pone.0179951>.
 77. Rosenkrantz AB, Sigmund EE, Winnick A, et al. Assessment of hepatocellular carcinoma using apparent diffusion coefficient and diffusion kurtosis indices: preliminary experience in fresh liver explants. *Magn Reson Imaging*. 2012;30:1534–40.
 78. Rosenkrantz AB, Sigmund EE, Johnson G, et al. Prostate cancer: feasibility and preliminary experience of a diffusional kurtosis model for detection and assessment of aggressiveness of peripheral zone cancer. *Radiology*. 2012;264:126–35.
 79. Yoshimaru D, Takatsu Y, Suzuki Y, Miyati T, Hamada Y, Funaki A, Tabata A, Maruyama C, Shimada M, Tobarai M, Nishino T. Diffusion kurtosis imaging in the assessment of liver function: Its potential as an effective predictor of liver function. *Br J Radiol*. 2019;92(1094):20170608. <https://doi.org/10.1259/bjr.20170608>.
 80. Argalia G, Tarantino G, Ventura C, Campioni D, Tagliati C, Guardati P, Kostandini A, Marzioni M, Giuseppe GM, Giovagnoni A. Shear wave elastography and transient elastography in HCV patients after direct-acting antivirals. *Radiol Med*. 2021. <https://doi.org/10.1007/s11547-020-01326-4>.
 81. Shin N, Choi JA, Choi JM, Cho ES, Kim JH, Chung JJ, Yu JS. Sclerotic changes of cavernous hemangioma in the cirrhotic liver: long-term follow-up using dynamic contrast-enhanced computed tomography. *Radiol Med*. 2020;125(12):1225–32. <https://doi.org/10.1007/s11547-020-01221-y>.
 82. Rampado O, Depaoli A, Marchisio F, Gatti M, Racine D, Ruggeri V, Ruggerello I, Darvizeh F, Fonio P, Popolo R. Effects of different levels of CT iterative reconstruction on low-contrast detectability and radiation dose in patients of different sizes: an anthropomorphic phantom study. *Radiol Med*. 2021;126(1):55–62. <https://doi.org/10.1007/s11547-020-01228-5>.
 83. Bottari A, Silipigni S, Carerj ML, Cattafi A, Maimone S, Marino MA, Mazziotti S, Pitrone A, Squadrato G, Ascenti G. Dual-source dual-energy CT in the evaluation of hepatic fractional extracellular space in cirrhosis. *Radiol Med*. 2020;125(1):7–14. <https://doi.org/10.1007/s11547-019-01089-7>.
 84. Izzo F, Granata V, Grassi R, Fusco R, Palaia R, Delrio P, Carrafiello G, Azoulay D, Petrillo A, Curley SA. Radiofrequency ablation and microwave ablation in Liver. *Oncologist*. 2019;24(10):e990–1005. <https://doi.org/10.1634/theoncologist.2018-0337>.
 85. Kuai ZX, Sang XQ, Yao YF, Chu CY, Zhu YM. Evaluation of non-exponential diffusion models for hepatocellular carcinoma using b values up to 2000 s/mm²: a short-term repeatability study. *J Magn Reson Imaging*. 2019;50(1):297–304. <https://doi.org/10.1002/jmri.26563>.
 86. Rosenkrantz AB, Sigmund EE, Winnick A, Niver BE, Spieler B, Morgan GR, et al. Assessment of hepatocellular carcinoma using apparent diffusion coefficient and diffusion kurtosis indices: preliminary experience in fresh liver explants. *Magn Reson Imaging*. 2012;30(10):1534–40. <https://doi.org/10.1016/j.mri.2012.04.020>.
 87. Goshima S, Kanematsu M, Noda Y, Kondo H, Watanabe H, Bae KT. Diffusion kurtosis imaging to assess response to treatment in hypervascular hepatocellular carcinoma. *AJR Am J Roentgenol*. 2015;204(5):W543–9. <https://doi.org/10.2214/AJR.14.13235>.
 88. Yilmaz C, Karaca CA, Iakobadze Z, Farajov R, Kilic K, Doganay L, et al. Factors affecting recurrence and survival after liver transplantation for hepatocellular carcinoma. *Transplant Proc*. 2018;50(10):3571–6. <https://doi.org/10.1016/j.transproceed.2018.05.027>.
 89. Poon RT, Fan ST, Lo CM, Liu CL, Wong J. Long-term survival and pattern of recurrence after resection of small hepatocellular carcinoma in patients with preserved liver function: implications for a strategy of salvage transplantation. *Ann Surg*. 2002;235(3):373–82. <https://doi.org/10.1097/0000658-200203000-00009>.
 90. Cicero G, Mazziotti S, Silipigni S, Blandino A, Cantisani V, Pergolizzi S, D'Angelo T, Stagno A, Maimone S, Squadrato G, Ascenti G. Dual-energy CT quantification of fractional extracellular space in cirrhotic patients: comparison between early and delayed equilibrium phases and correlation with oesophageal varices. *Radiol Med*. 2021. <https://doi.org/10.1007/s11547-021-01341-z>.
 91. Granata V, Fusco R, Catalano O, Guarino B, Granata F, Tatangelo F, Avallone A, Piccirillo M, Palaia R, Izzo F, Petrillo A. Intravoxel incoherent motion (IVIM) in diffusion-weighted imaging (DWI) for Hepatocellular carcinoma: correlation with histologic grade. *Oncotarget*. 2016;7(48):79357–64. <https://doi.org/10.18632/oncotarget.12689>.
 92. Cicero G, Ascenti G, Albrecht MH, Blandino A, Cavallaro M, D'Angelo T, Carerj ML, Vogl TJ, Mazziotti S. Extra-abdominal dual-energy CT applications: a comprehensive overview. *Radiol Med*. 2020;125:384–97. <https://doi.org/10.1007/s11547-019-01126-5>.
 93. Granata V, Fusco R, Venanzio Setola S, Sandomenico F, Luisa Barretta M, Belli A, Palaia R, Tatangelo F, Grassi R, Izzo F, Petrillo A. Major and ancillary features according to LI-RADS in the assessment of combined hepatocellular-cholangiocarcinoma. *Radiol Oncol*. 2020;54(2):149–58. <https://doi.org/10.2478/raon-2020-0029>.
 94. Granata V, Fusco R, Setola SV, Piccone C, Vallone P, Belli A, Incollongo P, Albino V, Tatangelo F, Izzo F, Petrillo A. Microvascular invasion and grading in hepatocellular carcinoma: correlation with major and ancillary features according to LI-RADS. *Abdom Radiol (NY)*. 2019;44(8):2788–800. <https://doi.org/10.1007/s00261-019-02056-6>.
 95. Cao L, Chen J, Duan T, Wang M, Jiang H, Wei Y, Xia C, Zhou X, Yan X, Song B. Diffusion kurtosis imaging (DKI) of hepatocellular carcinoma: correlation with microvascular invasion and histologic grade. *Quant Imaging Med Surg*. 2019;9(4):590–602. <https://doi.org/10.21037/qims.2019.02.14>.
 96. Wang GZ, Guo LF, Gao GH, Li Y, Wang XZ, Yuan ZG. Magnetic resonance diffusion kurtosis imaging versus diffusion-weighted imaging in evaluating the pathological grade of hepatocellular carcinoma. *Cancer Manag Res*. 2020;29(12):5147–58. <https://doi.org/10.2147/CMAR.S254371>.
 97. Granata V, Fusco R, Risi C, Ottaiano A, Avallone A, De Stefano A, Grimm R, Grassi R, Brunese L, Izzo F, Petrillo A. Diffusion-weighted MRI and diffusion kurtosis imaging to detect RAS mutation in colorectal liver metastasis. *Cancers (Basel)*. 2020;12(9):2420. <https://doi.org/10.3390/cancers12092420>.
 98. Nakamura Y, Higaki T, Honda Y, Tatsugami F, Tani C, Fukumoto W, Narita K, Kondo S, Akagi M, Awai K. Advanced CT techniques for assessing hepatocellular carcinoma. *Radiol Med*. 2021;126(7):925–35. <https://doi.org/10.1007/s11547-021-01366-4>.
 99. Fanelli F, Cannavale A, Chisci E, Citone M, Falcone GM, Michelagnoli S, Miele V. Direct percutaneous embolization of aneurysm sac: a safe and effective procedure to treat post-EVAR type II endoleaks. *Radiol Med*. 2021;126(2):258–63. <https://doi.org/10.1007/s11547-020-01247-2>.
 100. Minutoli F, Pergolizzi S, Blandino A, Mormina E, Amato E, Gaeta M. Effect of granulocyte colony-stimulating factor on bone marrow: evaluation by intravoxel incoherent motion and dynamic contrast-enhanced magnetic resonance imaging. *Radiol Med*. 2020;125(3):280–7. <https://doi.org/10.1007/s11547-019-01115-8>.
 101. Granata V, Grassi R, Fusco R, Setola SV, Belli A, Piccirillo M, Pradella S, Giordano M, Cappabianca S, Brunese L, Grassi R, Petrillo A, Izzo F. Abbreviated MRI protocol for the assessment of ablated area in HCC patients. *Int J Environ Res Public Health*. 2021;18(7):3598. <https://doi.org/10.3390/ijerph18073598>.
 102. Benedetti G, Mori M, Panzeri MM, Barbera M, Palumbo D, Sini C, Muffatti F, Andreasi V, Steidler S, Dogliani C, Partelli S, Manzoni M, Falconi M, Fiorino C, De Cobelli F. CT-derived radiomic features to discriminate histologic characteristics of pancreatic neuroendocrine tumors. *Radiol Med*. 2021;126(6):745–60. <https://doi.org/10.1007/s11547-021-01333-z>.
 103. Sun J, Yang L, Zhou Z, Zhang D, Han W, Zhang Q, Peng Y. Performance evaluation of two iterative reconstruction algorithms, MBIR and ASIR, in low radiation dose and low contrast dose abdominal CT in children. *Radiol Med*. 2020;125(10):918–25. <https://doi.org/10.1007/s11547-020-01191-1>.
 104. Higashi M, Tanabe M, Okada M, Furukawa M, Iida E, Ito K. Influence of fat deposition on T1 mapping of the pancreas: evaluation by dual-flip-angle MR imaging with and without fat suppression. *Radiol Med*. 2020;125(1):1–6. <https://doi.org/10.1007/s11547-019-01087-9>.
 105. Granata V, Fusco R, Bicchierai G, Cozzi D, Grazzini G, Danti G, De Muzio F, Maggioletti N, Smorchkova O, D'Elia M, Brunese MC, Grassi R, Giacobbe

- G, Bruno F, Palumbo P, Lacasella GV, Brunese L, Grassi R, Miele V, Barile A. Diagnostic protocols in oncology: workup and treatment planning. Part 1: the optimization of CT protocol. *Eur Rev Med Pharmacol Sci*. 2021;25(22):6972–94. https://doi.org/10.26355/eurev_202111_27246.
106. Granata V, Fusco R, Sansone M, Grassi R, Maio F, Palaia R, Tatangelo F, Botti G, Grimm R, Curley S, Avallone A, Izzo F, Petrillo A. Magnetic resonance imaging in the assessment of pancreatic cancer with quantitative parameter extraction by means of dynamic contrast-enhanced magnetic resonance imaging, diffusion kurtosis imaging and intravoxel incoherent motion diffusion-weighted imaging. *Therap Adv Gastroenterol*. 2020;21(13):1756284819885052. <https://doi.org/10.1177/1756284819885052>.
107. Shi YJ, Li XT, Zhang XY, Zhu HT, Liu YL, Wei YY, Sun YS. Non-gaussian models of 3-Tesla diffusion-weighted MRI for the differentiation of pancreatic ductal adenocarcinomas from neuroendocrine tumors and solid pseudopapillary neoplasms. *Magn Reson Imaging*. 2021;83:68–76. <https://doi.org/10.1016/j.mri.2021.07.006>.
108. Tafuto S, von Arx C, De Divitiis C, Maura CT, Palaia R, Albino V, Fusco R, Membrini M, Petrillo A, Granata V, Izzo F. ENETS center of excellence multidisciplinary group for neuroendocrine tumors in Naples (Italy). Electrochemotherapy as a new approach on pancreatic cancer and on liver metastases. *Int J Surg*. 2015;21(Suppl 1):78–82. <https://doi.org/10.1016/j.ijsu.2015.04.095>.
109. Granata V, Fusco R, Piccirillo M, Palaia R, Petrillo A, Lastoria S, Izzo F. Electrochemotherapy in locally advanced pancreatic cancer: preliminary results. *Int J Surg*. 2015;18:230–6. <https://doi.org/10.1016/j.ijsu.2015.04.055>.
110. Izzo F, Granata V, Fusco R, D'Alessio V, Petrillo A, Lastoria S, Piccirillo M, Albino V, Belli A, Tafuto S, Avallone A, Patrone R, Palaia R. Clinical phase I/II study: local disease control and survival in locally advanced pancreatic cancer treated with electrochemotherapy. *J Clin Med*. 2021;10(6):1305. <https://doi.org/10.3390/jcm10061305>.
111. Granata V, Fusco R, D'Alessio V, Giannini A, Venanzio Setola S, Belli A, Palaia R, Petrillo A, Izzo F. Electroporation-based treatments in minimally invasive percutaneous, laparoscopy and endoscopy procedures for treatment of deep-seated tumors. *Eur Rev Med Pharmacol Sci*. 2021;25(9):3536–45. https://doi.org/10.26355/eurev_202105_25836.
112. Rega D, Granata V, Petrillo A, Pace U, Sassaroli C, Di Marzo M, Cervone C, Fusco R, D'Alessio V, Nasti G, Romano C, Avallone A, Pecori B, Botti G, Tatangelo F, Maiolino P, Delrio P. Organ sparing for locally advanced rectal cancer after neoadjuvant treatment followed by electrochemotherapy. *Cancers (Basel)*. 2021;13(13):3199. <https://doi.org/10.3390/cancers13133199>.
113. Granata V, Fusco R, Setola SV, Piccirillo M, Leongito M, Palaia R, Granata F, Lastoria S, Izzo F, Petrillo A. Early radiological assessment of locally advanced pancreatic cancer treated with electrochemotherapy. *World J Gastroenterol*. 2017;23(26):4767–78. <https://doi.org/10.3748/wjg.v23.i26.4767>.
114. Granata V, Fusco R, Setola SV, Palaia R, Albino V, Piccirillo M, Grimm R, Petrillo A, Izzo F. Diffusion kurtosis imaging and conventional diffusion weighted imaging to assess electrochemotherapy response in locally advanced pancreatic cancer. *Radiol Oncol*. 2019;53(1):15–24. <https://doi.org/10.2478/raon-2019-0004>.
115. Rega D, Granata V, Romano C, D'Angelo V, Pace U, Fusco R, Cervone C, Ravo V, Tatangelo F, Avallone A, Petrillo A, Delrio P. Watch and wait approach for rectal cancer following neoadjuvant treatment: the experience of a high volume cancer center. *Diagnostics (Basel)*. 2021;11(8):1507. <https://doi.org/10.3390/diagnostics11081507>.
116. Schicchi N, Fogante M, Palumbo P, Agliata G, Esposto Pirani P, Di Cesare E, Giovagnoni A. The sub-millisievert era in CTCA: the technical basis of the new radiation dose approach. *Radiol Med*. 2020;125(11):1024–39. <https://doi.org/10.1007/s11547-020-01280-1>.
117. Granata V, Grassi R, Fusco R, Izzo F, Brunese L, Delrio P, Avallone A, Pecori B, Petrillo A. Current status on response to treatment in locally advanced rectal cancer: what the radiologist should know. *Eur Rev Med Pharmacol Sci*. 2020;24(23):12050–62. https://doi.org/10.26355/eurev_202012_23994.
118. Park SH, Kim YS, Choi J. Dosimetric analysis of the effects of a temporary tissue expander on the radiotherapy technique. *Radiol Med*. 2021;126(3):437–44. <https://doi.org/10.1007/s11547-020-01297-6>.
119. Crimi F, Capelli G, Spolverato G, Bao QR, Florio A, Milite Rossi S, Cecchin D, Albertoni L, Campi C, Pucciarelli S, Stramare R. MRI T2-weighted sequences-based texture analysis (TA) as a predictor of response to neoadjuvant chemo-radiotherapy (nCRT) in patients with locally advanced rectal cancer (LARC). *Radiol Med*. 2020;125(12):1216–24. <https://doi.org/10.1007/s11547-020-01215-w>.
120. Bertocchi E, Barugola G, Nicosia L, Mazzola R, Ricchetti F, Dell'Abate P, Alongi F, Ruffo G. A comparative analysis between radiation dose intensification and conventional fractionation in neoadjuvant locally advanced rectal cancer: a monocentric prospective observational study. *Radiol Med*. 2020;125:990–8. <https://doi.org/10.1007/s11547-020-01189-9>.
121. Fornell-Perez R, Vivas-Escalona V, Aranda-Sanchez J, Gonzalez-Dominguez MC, Rubio-Garcia J, Aleman-Flores P, Lozano-Rodriguez A, Porcel-de-Peralta G, Loro-Ferrer JF. Primary and post-chemoradiotherapy MRI detection of extramural venous invasion in rectal cancer: the role of diffusion-weighted imaging. *Radiol Med*. 2020;125(6):522–30. <https://doi.org/10.1007/s11547-020-01137-7>.
122. Cusumano D, Meijer G, Lenkiewicz J, Chiloilo G, Boldrini L, Masciocchi C, Dinapoli N, Gatta R, Casà C, Damiani A, Barbaro B, Gambacorta MA, Azario L, De Spirito M, Intven M, Valentini V. A field strength independent MR radiomics model to predict pathological complete response in locally advanced rectal cancer. *Radiol Med*. 2021;126(3):421–9. <https://doi.org/10.1007/s11547-020-01266-z>.
123. Fusco R, Sansone M, Granata V, Grimm R, Pace U, Delrio P, Tatangelo F, Botti G, Avallone A, Pecori B, Petrillo A. Diffusion and perfusion MR parameters to assess preoperative short-course radiotherapy response in locally advanced rectal cancer: a comparative explorative study among standardized index of shape by DCE-MRI, intravoxel incoherent motion- and diffusion kurtosis imaging-derived parameters. *Abdom Radiol (NY)*. 2019;44(11):3683–700. <https://doi.org/10.1007/s00261-018-1801-z>.
124. Granata V, Caruso D, Grassi R, Cappabianca S, Reginelli A, Rizzati R, Masselli G, Golfieri R, Rengo M, Regge D, Lo Re G, Pradella S, Fusco R, Faggioni L, Laghi A, Miele V, Neri E, Coppola F. Structured reporting of rectal cancer staging and restaging: a consensus proposal. *Cancers (Basel)*. 2021;13(9):2135. <https://doi.org/10.3390/cancers13092135>.
125. Granata V, Fusco R, Reginelli A, Delrio P, Selvaggi F, Grassi R, Izzo F, Petrillo A. Diffusion kurtosis imaging in patients with locally advanced rectal cancer: current status and future perspectives. *J Int Med Res*. 2019;47(6):2351–60. <https://doi.org/10.1177/0300060519827168>.
126. Petrillo A, Fusco R, Granata V, Filice S, Sansone M, Rega D, Delrio P, Bianco F, Romano GM, Tatangelo F, Avallone A, Pecori B. Assessing response to neo-adjuvant therapy in locally advanced rectal cancer using intra-voxel incoherent motion modelling by DWI data and standardized index of shape from DCE-MRI. *Ther Adv Med Oncol*. 2018;16(10):1758835918809875. <https://doi.org/10.1177/1758835918809875>.
127. Fusco R, Granata V, Rega D, Russo C, Pace U, Pecori B, Tatangelo F, Botti G, Izzo F, Cascella M, Avallone A, Delrio P, Petrillo A. Morphological and functional features prognostic factor of magnetic resonance imaging in locally advanced rectal cancer. *Acta Radiol*. 2019;60(7):815–25. <https://doi.org/10.1177/0284185118803783>.
128. Petrillo A, Fusco R, Petrillo M, Granata V, Bianco F, Di Marzo M, Delrio P, Tatangelo F, Botti G, Pecori B, Avallone A. DCE-MRI time-intensity curve visual inspection to assess pathological response after neoadjuvant therapy in locally advanced rectal cancer. *Jpn J Radiol*. 2018;36(10):611–21. <https://doi.org/10.1007/s11604-018-0760-1>.
129. Petrillo A, Fusco R, Granata V, Setola SV, Sansone M, Rega D, Delrio P, Bianco F, Romano GM, Tatangelo F, Avallone A, Pecori B. MR imaging perfusion and diffusion analysis to assess preoperative short course radiotherapy response in locally advanced rectal cancer: standardized index of shape by DCE-MRI and intravoxel incoherent motion-derived parameters by DW-MRI. *Med Oncol*. 2017;34(12):198. <https://doi.org/10.1007/s12032-017-1059-2>.
130. Fusco R, Petrillo M, Granata V, Filice S, Sansone M, Catalano O, Petrillo A. Magnetic resonance imaging evaluation in neoadjuvant therapy of locally advanced rectal cancer: a systematic review. *Radiol Oncol*. 2017;51(3):252–62. <https://doi.org/10.1515/raon-2017-0032>.
131. Reginelli A, Granata V, Fusco R, Granata F, Rega D, Roberto L, Pel-lino G, Rotondo A, Selvaggi F, Izzo F, Petrillo A, Grassi R. Diagnostic

- performance of magnetic resonance imaging and 3D endoanal ultrasound in detection, staging and assessment post treatment, in anal cancer. *Oncotarget*. 2017;8(14):22980–90. <https://doi.org/10.18632/oncotarget.14946>.
132. Petrillo A, Fusco R, Petrillo M, Granata V, Delrio P, Bianco F, Pecori B, Botti G, Tatangelo F, Caracò C, Aloj L, Avallone A, Lastoria S. Standardized index of shape (DCE-MRI) and standardized uptake value (PET/CT): two quantitative approaches to discriminate chemo-radiotherapy locally advanced rectal cancer responders under a functional profile. *Oncotarget*. 2017;8(5):8143–53. <https://doi.org/10.18632/oncotarget.14106>.
 133. Zhu L, Pan Z, Ma Q, et al. Diffusion kurtosis imaging study of rectal adenocarcinoma associated with histopathologic prognostic factors: preliminary findings. *Radiology*. 2017;284:66–76. <https://doi.org/10.1148/radiol.2016160094>.
 134. Cui Y, Yang X, Du X, et al. Whole-tumour diffusion kurtosis MR imaging histogram analysis of rectal adenocarcinoma: correlation with clinical pathologic prognostic factors. *Eur Radiol*. 2018;28:1485–94. <https://doi.org/10.1007/s00330-017-5094-3>.
 135. Yu J, Dai X, Zou HH, et al. Diffusion kurtosis imaging in identifying the malignancy of lymph nodes during the primary staging of rectal cancer. *Colorectal Dis*. 2018;20:116–25. <https://doi.org/10.1111/codi.13835>.
 136. Yu J, Huang DY, Li Y, et al. Correlation of standard diffusion-weighted imaging and diffusion kurtosis imaging with distant metastases of rectal carcinoma. *J Magn Reson Imaging*. 2016;44:221–9. <https://doi.org/10.1002/jmri.25137>.
 137. Yu J, Xu Q, Song JC, et al. The value of diffusion kurtosis magnetic resonance imaging for assessing treatment response of neo-adjuvant chemoradiotherapy in locally advanced rectal cancer. *Eur Radiol*. 2017;27:1848–57. <https://doi.org/10.1007/s00330-016-4529-6>.
 138. Hu F, Tang W, Sun Y, et al. The value of diffusion kurtosis imaging in assessing pathological complete response to neoadjuvant chemoradiation therapy in rectal cancer: a comparison with conventional diffusion-weighted imaging. *Oncotarget*. 2017;8:75597–606. <https://doi.org/10.18632/oncotarget.17491>.
 139. Petralia G, Zugni F, Summers PE, Colombo A, Pricolo P, Grazioli L, Colagrande S, Giovagnoni A, Padhani AR. Italian working group on magnetic resonance. Whole-body magnetic resonance imaging (WB-MRI) for cancer screening: recommendations for use. *Radiol Med*. 2021;126(11):1434–50.
 140. Petralia G, Summers PE, Agostini A, Ambrosini R, Cianci R, Cristel G, Calistri L, Colagrande S. Dynamic contrast-enhanced MRI in oncology: how we do it. *Radiol Med*. 2020;125(12):1288–300. <https://doi.org/10.1007/s11547-020-01220-z>.
 141. Halefoglu AM, Ozagari AA. Tumor grade estimation of clear cell and papillary renal cell carcinomas using contrast-enhanced MDCT and FSE T2 weighted MR imaging: radiology-pathology correlation. *Radiol Med*. 2021;126(9):1139–48. <https://doi.org/10.1007/s11547-021-01350-y>.
 142. Greco F, Mallio CA. Relationship between visceral adipose tissue and genetic mutations (VHL and KDM5C) in clear cell renal cell carcinoma. *Radiol Med*. 2021;126(5):645–51. <https://doi.org/10.1007/s11547-020-01310-y>.
 143. Tsili AC, Andriotis E, Gkeli MG, Krokidis M, Stasinopoulou M, Varkarakis IM, Mouloupoulos LA. Oncologic imaging subcommittee working group of the hellenic radiological society. The role of imaging in the management of renal masses. *Eur J Radiol*. 2021;141:109777. <https://doi.org/10.1016/j.ejrad.2021.109777>.
 144. Ciccarese F, Brandi N, Corcioni B, Golfieri R, Gaudiano C. Complicated pyelonephritis associated with chronic renal stone disease. *Radiol Med*. 2021;126(4):505–16. <https://doi.org/10.1007/s11547-020-01315-7>.
 145. Hongyo H, Higashihara H, Osuga K, Kashiwagi E, Kosai S, Nagai K, Tanaka K, Ono Y, Ujike T, Uemura M, Imamura R, Nonomura N, Tomiyama N. Efficacy of prophylactic selective arterial embolization for renal angio-myliomas: identifying predictors of 50% volume reduction. *CVIR Endovasc*. 2020;3(1):84. <https://doi.org/10.1186/s42155-020-00179-2>.
 146. Yap FY, Varghese BA, Cen SY, Hwang DH, Lei X, Desai B, Lau C, Yang LL, Fullenkamp AJ, Hajian S, Rivas M, Gupta MN, Quinn BD, Aron M, Desai MM, Aron M, Oberai AA, Gill IS, Duddalwar VA. Shape and texture-based radiomics signature on CT effectively discriminates benign from malignant renal masses. *Eur Radiol*. 2021;31(2):1011–21. <https://doi.org/10.1007/s00330-020-07158-0>.
 147. Allgood E, Raman SS. Image interpretation: practical triage of benign from malignant renal masses. *Radiol Clin North Am*. 2020;58(5):875–84. <https://doi.org/10.1016/j.rcl.2020.06.002>.
 148. Nazari M, Shiri I, Hajianfar G, Oveisi N, Abdollahi H, Deevband MR, Oveisi M, Zaidi H. Noninvasive Fuhrman grading of clear cell renal cell carcinoma using computed tomography radiomic features and machine learning. *Radiol Med*. 2020;125(8):754–62. <https://doi.org/10.1007/s11547-020-01169-z>.
 149. Greco F, Mallio CA, Grippo R, Messina L, Vallesse S, Rabitti C, Quarta LG, Grasso RF, Beomonte ZB. Increased visceral adipose tissue in male patients with non-clear cell renal cell carcinoma. *Radiol Med*. 2020;125(6):538–43. <https://doi.org/10.1007/s11547-020-01146-6>.
 150. Curci NE. On high grade kidney cancer and machine learning. *Acad Radiol*. 2020;27(2):169–70. <https://doi.org/10.1016/j.acra.2019.10.009>.
 151. Asayama Y, Nishie A, Ushijima Y, Okamoto D, Morita K, Takao S, Kakiyama D, Ishimatsu K, Ishigami K, Fujita N, Honda H. Usefulness of a pretreatment CT-based modified RENAL nephrometry score in predicting renal function after cryotherapy for T1a renal mass. *Cardiovasc Intervent Radiol*. 2019;42(8):1128–34. <https://doi.org/10.1007/s00270-019-02238-1>.
 152. Ding Y, Tan Q, Mao W, Dai C, Hu X, Hou J, Zheng M, Zhou J. Differentiating between malignant and benign renal tumors: do IVIM and diffusion kurtosis imaging perform better than DWI. *Eur Radiol*. 2019;29(12):6930–9.
 153. Fu J, Ye J, Zhu W, Wu J, Chen W, Zhu Q. Magnetic resonance diffusion kurtosis imaging in differential diagnosis of benign and malignant renal tumors. *Cancer Imaging*. 2021;21(1):6. <https://doi.org/10.1186/s40644-020-00369-0>.
 154. Zhu J, Luo X, Gao J, Li S, Li C, Chen M. Application of diffusion kurtosis tensor MR imaging in characterization of renal cell carcinomas with different pathological types and grades. *Cancer Imaging*. 2021;21(1):30. <https://doi.org/10.1186/s40644-021-00394-7>.
 155. Cao J, Luo X, Zhou Z, Duan Y, Xiao L, Sun X, Shang Q, Gong X, Hou Z, Kong D, He B. Comparison of diffusion-weighted imaging mono-exponential mode with diffusion kurtosis imaging for predicting pathological grades of clear cell renal cell carcinoma. *Eur J Radiol*. 2020;130:109195. <https://doi.org/10.1016/j.ejrad.2020.109195>.
 156. Nardone V, Reginelli A, Grassi R, Boldrini L, Vacca G, D'Ippolito E, Annunziata S, Farchione A, Belfiore MP, Desideri I, Cappabianca S. Delta radiomics: a systematic review. *Radiol Med*. 2021;126(12):1571–83. <https://doi.org/10.1007/s11547-021-01436-7>.
 157. Fusco R, Sansone M, Granata V, Setola SV, Petrillo A. A systematic review on multiparametric MR imaging in prostate cancer detection. *Infect Agent Cancer*. 2017;30(12):57. <https://doi.org/10.1186/s13027-017-0168-z>.
 158. Fusco R, Sansone M, Petrillo M, Setola SV, Granata V, Botti G, Perdonà S, Borzillo V, Muto P, Petrillo A. Multiparametric MRI for prostate cancer detection: preliminary results on quantitative analysis of dynamic contrast enhanced imaging, diffusion-weighted imaging and spectroscopy imaging. *Magn Reson Imaging*. 2016;34(7):839–45. <https://doi.org/10.1016/j.mri.2016.04.001>.
 159. Petrillo A, Fusco R, Setola SV, Ronza FM, Granata V, Petrillo M, Carone G, Sansone M, Franco R, Fulciniti F, Perdonà S. Multiparametric MRI for prostate cancer detection: performance in patients with prostate-specific antigen values between 2.5 and 10 ng/mL. *J Magn Reson Imaging*. 2014;39(5):1206–12. <https://doi.org/10.1002/jmri.24269>.
 160. Boschheidgen M, Schimmöller L, Arsov C, Ziaee F, Morawitz J, Valentin B, Radke KL, Giessing M, Esposito I, Albers P, Antoch G, Ullrich T. MRI grading for the prediction of prostate cancer aggressiveness. *Eur Radiol*. 2021. <https://doi.org/10.1007/s00330-021-08332-8>.
 161. Coppola A, Platania G, Ticca C, De Mattia C, Bortolato B, Palazzi MF, Vanzulli A. Sensitivity of CE-MRI in detecting local recurrence after radical prostatectomy. *Radiol Med*. 2020;125(7):683–90. <https://doi.org/10.1007/s11547-020-01149-3>.
 162. Cutaia G, Tosto G, Cannella R, Bruno A, Leto C, Salvaggio L, Cutaia S, Lombardo FP, Dispensa N, Giambelluca D, Midiri M, Salvaggio G. Prevalence and clinical significance of incidental findings on multiparametric prostate MRI. *Radiol Med*. 2020;125(2):204–13. <https://doi.org/10.1007/s11547-019-01106-9>.

163. Ediz SS, Gunduz N. The relationship between PI-RADS categories and incidental findings in multiparametric prostate MRI. *J Coll Phys Surg Pak*. 2021;31(9):1030–4. <https://doi.org/10.29271/jcpsp.2021.09.1030>.
164. Rosenkrantz AB, Sigmund EE, Johnson G, et al. Prostate cancer: feasibility and preliminary experience of a diffusional kurtosis model for detection and assessment of aggressiveness of peripheral zone cancer. *Radiology*. 2012;264:126–35.
165. Suo S, Chen X, Wu L, et al. Non-gaussian water diffusion kurtosis imaging of prostate cancer. *Magn Reson Imaging*. 2014;32:421–7.
166. Wang Q, Li H, Yan X, et al. Histogram analysis of diffusion kurtosis magnetic resonance imaging in differentiation of pathologic Gleason grade of prostate cancer. *Urol Oncol*. 2015;33(337):e15–24.
167. Roethke MC, Kuder TA, Kuru TH, et al. Evaluation of diffusion kurtosis imaging versus standard diffusion imaging for detection and grading of peripheral zone prostate cancer. *Invest Radiol*. 2015;50:483–9.
168. Toivonen J, Merisaari H, Pesola M, et al. Mathematical models for diffusion-weighted imaging of prostate cancer using b values up to 2000 s/mm²: correlation with Gleason score and repeatability of region of interest analysis. *Magn Reson Med*. 2015;74:1116–24.
169. Tamada T, Prabhu V, Li J, et al. Diffusion-weighted MR imaging for detection and assessment of aggressiveness—comparison between conventional and kurtosis models. *Radiology*. 2017;284:100–8.
170. Hou M, Song K, Ren J, Wang K, Guo J, Niu Y, Li Z, Han D. Comparative analysis of the value of amide proton transfer-weighted imaging and diffusion kurtosis imaging in evaluating the histological grade of cervical squamous carcinoma. *BMC Cancer*. 2022;22(1):87. <https://doi.org/10.1186/s12885-022-09205-z>.
171. Chen T, Li Y, Lu SS, Zhang YD, Wang XN, Luo CY, Shi HB. Quantitative evaluation of diffusion-kurtosis imaging for grading endometrial carcinoma: a comparative study with diffusion-weighted imaging. *Clin Radiol*. 2017;72(11):995.e11–995.e20. <https://doi.org/10.1016/j.crad.2017.07.004>.
172. Yue W, Meng N, Wang J, Liu W, Wang X, Yan M, Han D, Cheng J. Comparative analysis of the value of diffusion kurtosis imaging and diffusion-weighted imaging in evaluating the histological features of endometrial cancer. *Cancer Imaging*. 2019;19(1):9. <https://doi.org/10.1186/s40644-019-0196-6>.
173. Zhang A, Song J, Ma Z, Chen T. Combined dynamic contrast-enhanced magnetic resonance imaging and diffusion-weighted imaging to predict neoadjuvant chemotherapy effect in FIGO stage IB2-IIA2 cervical cancers. *Radiol Med*. 2020;125(12):1233–42. <https://doi.org/10.1007/s11547-020-01214-x>.
174. Russo L, Gui B, Miccò M, Panico C, De Vincenzo R, Fanfani F, Scambia G, Manfredi R. The role of MRI in cervical cancer > 2 cm (FIGO stage IB2-IIA1) conservatively treated with neoadjuvant chemotherapy followed by conization: a pilot study. *Radiol Med*. 2021;126(8):1055–63. <https://doi.org/10.1007/s11547-021-01377-1>.
175. Albano D, Stecco A, Micci G, Sconfienza LM, Colagrande S, Reginelli A, Grassi R, Carriero A, Midiri M, Lagalla R, Galia M. Whole-body magnetic resonance imaging (WB-MRI) in oncology: an Italian survey. *Radiol Med*. 2021;126(2):299–305. <https://doi.org/10.1007/s11547-020-01242-7>.
176. Ria F, Samei E. Is regulatory compliance enough to ensure excellence in medicine? *Radiol Med*. 2020;125:904–5. <https://doi.org/10.1007/s11547-020-01171-5>.
177. Scapicchio C, Gabelloni M, Barucci A, Cioni D, Saba L, Neri E. A deep look into radiomics. *Radiol Med*. 2021;126(10):1296–311. <https://doi.org/10.1007/s11547-021-01389-x>.
178. Nougaret S, Horta M, Sala E, Lakhman Y, Thomassin-Naggara I, Kido A, Masselli G, Bharwani N, Sadowski E, Ertmer A, Otero-Garcia M, Kubik-Huch RA, Cunha TM, Rockall A, Forstner R. Endometrial cancer MRI staging: updated guidelines of the European society of urogenital radiology. *Eur Radiol*. 2019;29:792–805.
179. Kinkel K, Forstner R, Danza FM, Oleaga L, Cunha TM, Bergman A, Barentsz JO, Balleyguier C, Brkljacic B, Spencer JA. European society of urogenital imaging. Staging of endometrial cancer with MRI: guidelines of the European society of Urogenital Imaging. *Eur Radiol*. 2009;19:1565–74.
180. Mori N, Mugikura S, Takase K. Importance of ADC parameters from histogram analysis corresponding to histological components in endometrial cancer. *Eur J Radiol*. 2021;144:110004. <https://doi.org/10.1016/j.ejrad.2021.110004>.
181. Levine EM, Fernandez CM. Determining the stage of endometrial cancer for its surgical treatment. *Am J Obstet Gynecol*. 2022. <https://doi.org/10.1016/j.ajog.2022.02.014>.
182. Ding H, Jiang F, Deng L, Wang J, Wang P, Ji M, Li J, Shi W, Pei Y, Li J, Zhang Y, Zhang Z, Chen Y, Li B. Prediction of clinical outcome in endometrial carcinoma based on a 3-lncRNA signature. *Front Cell Dev Biol*. 2022;1(9):814456. <https://doi.org/10.3389/fcell.2021.814456>.

Publisher's Note

Springer Nature remains neutral with regard to jurisdictional claims in published maps and institutional affiliations.

Ready to submit your research? Choose BMC and benefit from:

- fast, convenient online submission
- thorough peer review by experienced researchers in your field
- rapid publication on acceptance
- support for research data, including large and complex data types
- gold Open Access which fosters wider collaboration and increased citations
- maximum visibility for your research: over 100M website views per year

At BMC, research is always in progress.

Learn more biomedcentral.com/submissions

